

Deciphering role of inter and intracity human dispersal on epidemic spread via coupled reaction-diffusion models

M.A. Aziz-Alaoui · Parimita Roy

Received: date / Accepted: date

Abstract Public health has been significantly influenced by human mobility patterns since time immemorial. A susceptible-infected-deceased epidemic reaction diffusion network model using asymptotic transmission rate is proposed to portray the spatial spread of the epidemic among two cities due to population dispersion. Qualitative behaviour including global attractor and persistence property are obtained. We also study asymptotic behaviour of the whole network with the help of asymptotic behaviour at individual cities. The epidemic model shows up two equilibria, (i) the disease-free, and (ii) unique endemic equilibria. An expression that can be used to calculate the basic reproduction number for heterogeneous environment, for the entire network is obtained. We use graph theory to analyze the global stability of our diffusive two-city model. We also performed bifurcation analysis and found that endemic equilibrium changes stability via Hopf bifurcations. A significant reduction in infection cases were observed when proper migration rate is maintained between the cities. Numerical results are provided to illuminate and clarify theoretical findings. Simulation experiments for two-dimensional spatial model shows that infectious population will increase if contact heterogeneity is increased, but it will decline if infective population performs more local random movement. We observe that infection risk may be understated if the parameters used to estimate the basic reproduction number are kept constant.

Keywords Reaction-diffusion · Heterogeneity · Global stability · Reproduction number · Pattern formation

1 Introduction

In the long history of mankind, infectious disease has a deep effect on human populations, including their development and evolution. Individual's health status is affected by many factors, such as the quantity of time spent in a specific place, availability and access to affordable health care, complex economic and social factors, educational attainments, and lifestyles. Despite significant advances in medical sciences, infectious disease affects both the human and animal population in many parts of the world. Since performing experiments on the population is prohibited one can use mathematical model to investigate the transmission, predict the outbreak and even control of epidemics [2]. At

M.A. Aziz-Alaoui
Normandie Univ, UNIHAVRE, LMAH, FR-CNRS-3335, ISCN, 76600 Le Havre, France
Tel.: +33-670737669
Fax: +33-232744314
E-mail: aziz.alaoui1@gmail.com

Corresponding Author: Parimita Roy
Normandie Univ, UNIHAVRE, LMAH, FR-CNRS-3335, ISCN, 76600 Le Havre, France
and School of Mathematics,
Thapar institute of Engineering and Technology,
Patiala, Punjab
E-mail: parimita.roy@thapar.edu

present, mathematical models are considered as one of the active topic in public health and biology to determine whether the epidemics can be broken out or not [38]. Many real-world systems often interact and influence each other. The relationship between migration and the introduction of disease has been recognized in epidemiology for a long duration. There are many Ordinary differential equation models constructed to study the effect of the spatial heterogeneity and migration on disease transmission, which uses meta-population models ([16], [19], [14]). Hethcote (1976) [15] proposed two-patch epidemic model with population dispersal. Wang and Zhao (2004) [56] and references therein also described the dynamics of disease propagation between different patches due to population dispersal. These studies consider meta-population models, in which the population are subdivided into distinct patches, each of which are considered as homogeneous. This model formulation process is frequently used for understanding the transmission of disease between and within different population centers. One can use these models to examine the spatial dynamics of city-by-city transmission and to investigate the reason for high levels of synchronicity observed between town, cities, and so forth during disease outbreaks.

Another emerging field that is widely studied to investigate epidemic spreading, including rumours, human disease and computer viruses is complex network models. Complex network is a new branch in statistical physics which provides a reliable model for the intensive study of the epidemic spreading. In complex network modelling nodes represent individuals or organization and link the interactions among them. Mathematical analysis of such models have revealed the importance of topology for investigating propagation dynamics. Liu et al. (2010) [34], Wen-Jie and Xing-Yuan (2013) [62] studied the epidemic spreading and discussed the credibility of homogeneous mixing hypothesis. Ren and Wang (2014) [47] proposed a network model with time-varying community structure. They found that the time of the epidemic outbreak depends mainly on the mobility rate of the individual. Wen-Jie and Yuan [60] proposed a novel model with two strategies for controlling epidemic disease: quarantine and message delivery. Nian et al. (2018) [41] constructed a dynamic network model based on Barabasi-Albert (BA), keeping the same total number of edges. They showed immunization based on node activity is effective and is more feasible in dynamic networks. Wang and Zhao (2017) [59] generalized the susceptible-Infected-Susceptible (SIS) model that explores the propagation of multi-messages by considering their correlation degree. These models provided very powerful results but did not display the complete local and global spatial spread dynamics.

These researches are enlightened to our work, yet most of them are focused on static network models. However, in reality our life is not static. We move from one city to another to perform our job etc. and then we come back to our own city and perform local random movement. The major drawback of these models is that they do not include spatial heterogeneity and local random movement which can also affect the spread of epidemics. The heterogeneity of the spatial environment is considered as an important contributing factor in propagating many contagious diseases. This is barely surprising as populations in actuality are not homogeneous: interactions between individuals are likely to have limited scope. As spatial spread of disease relies on complex interaction between distinct elements (like, diverse nature of a given population and the dynamics innate to a given pathogen/host interaction), mathematical models provide a quality conceptual structure with which spatial emergence of patterns and processes involved can be studied and explained. In modeling geographic effects or spatial dispersal of a disease, a discrimination is usually created between dispersal and diffusion models. Using partial differential equations, one can typically introduce spatial variation in epidemic models. A reaction–diffusion (RD) model describes the proliferation (reaction) and movement (diffusion) of individuals. By diffusion model, dissemination of infection to immediate adjoining neighbours can be studied. This mechanical–biological interaction within and surrounding cells has been previously incorporated into modelling cancer of brain, breast, kidney and pancreatic. Here, we apply it to model spread of disease among two connected cities using a mechanically coupled RD model. The spatial spread of diseases like influenza [64], Ebola involves many unusual and distinct components. Therefore, modeling their spread is a complicated task.

The propagation of global pandemic diseases are affected by transportation, and is considered as one of the relevant and crucial problems on the epidemiological multi-group models. Over the last forty years, both the scope and process of migration have experienced significant shifts, and the majority of these changes have transformed the innate characteristics of migration-accompanied infectious disease. In this paper, an effort has been made to decipher the effect of migration on epidemic spread among heterogeneous cities coupled through reaction-diffusion modeling. The aim is to recommend some preventive health-policy measures during an outbreak. Asymptotic infection rate which displays

a saturation effect have been rarely considered for network reaction-diffusion modeling [10]. The asymptotic infection rate, $\frac{\beta I}{S+I+c}$, is a function of the number of infections present at a given point of time. This signifies the fact that the number of contacts an individual carrying the virus can have with other individuals reaches some finite maximum value due to the spatial or social distribution of the population and/or limitation of time. We believe that this is the first work that considers a two-patch reaction-diffusion epidemiological model to mimic the scenario of intra and intercity human dispersal. We also computed basic reproduction numbers for coupled reaction-diffusion systems. We emphasize that this rate and heterogeneous transmission rate has significant contributions to the dynamics of disease spread. **Our mathematical analysis are inspired by [8], [17], [9], [22], [26], [27], [28], [30], [31], [44], [51], [61], [63].**

The manuscript is organized as follows: In section 2 two-city susceptible-infected-deceased (SID) model with global and local movement is formulated. In section 3, the existence of equilibrium is analysed and reproduction number is calculated. Global stability using graph theory is discussed in section 4. Numerical results are presented to confirm the analytical findings in section 5. In section 6, we summarize the main contributions of the work.

2 Formulation of Epidemic Model

In the model introduced by Upadhyay et al. (2014) [55], there is no intercity travel. Communicable diseases such as sexual diseases and influenza can be passed on easily from one city to other cities. Therefore, considering the effect of both local (within city) and global (across city) population dispersal on the spread of epidemics are relevant and important. In this work, we considered two city models which are connected by road. We do not care about the dynamics taking place in connecting roads. A typical disease is captured by the following Susceptible-Infected-Deceased structure modelling.

$$\begin{aligned}\frac{dS}{dt} &= rS \left(1 - \frac{S+I}{K}\right) - \frac{\beta SI}{S+I+c}, \\ \frac{dI}{dt} &= \frac{\beta SI}{S+I+c} - aI, \\ \frac{dD}{dt} &= aI.\end{aligned}$$

We omit the equation D for further calculation since the above system does not depend on D . The following assumptions are taken into account while formulating the two city epidemiological model:

- (i) We considered a population that is structured and interacting in two cities.
- (ii) Let (S_1, I_1) and (S_2, I_2) denotes the density of susceptible and infective individuals resident in city 1 and city 2 respectively.
- (iii) The disease is transmitted to a susceptible individual by an effective contact with an infected individual.
- (iv) We use asymptotic transmission incidence to model disease transmission phenomenon, which, for human is considered more accurate than mass action ([10], [39], [55]).
- (v) The virus is spread among the population only and the disease is not inherited genetically.
- (vi) During travelling there is no birth or death.

Considering above assumptions the epidemic situation in two cities with bidirectional movement can be modeled by the following system of differential equation,

$$\frac{dS_1}{dt} = r_1 S_1 \left(1 - \frac{S_1 + I_1}{K_1}\right) - \frac{\beta_1 S_1 I_1}{S_1 + I_1 + c_1} + m_1 S_2 - m_2 S_1 = f_1(S_1, I_1) + m_1 S_2 - m_2 S_1, \quad (1)$$

$$\frac{dI_1}{dt} = \frac{\beta_1 S_1 I_1}{S_1 + I_1 + c_1} - a_1 I_1 + m_3 I_2 - m_4 I_1 = f_2(S_1, I_1) + m_3 I_2 - m_4 I_1, \quad (2)$$

$$\frac{dS_2}{dt} = r_2 S_2 \left(1 - \frac{S_2 + I_2}{K_2}\right) - \frac{\beta_2 S_2 I_2}{S_2 + I_2 + c_2} + m_2 S_1 - m_1 S_2 = f_3(S_2, I_2) + m_2 S_1 - m_1 S_2, \quad (3)$$

$$\frac{dI_2}{dt} = \frac{\beta_2 S_2 I_2}{S_2 + I_2 + c_2} - a_2 I_2 + m_4 I_1 - m_3 I_2 = f_4(S_2, I_2) + m_4 I_1 - m_3 I_2. \quad (4)$$

All the parameters appearing in (1)-(4) are assumed to be positive constants. A concise description about (1)-(4) system parameters and variables is presented in Table 1.

Further, we suppose that functions S_1, I_1, S_2, I_2 depend on time as well as on space. The heterogeneity in space and the local movement of individuals plays a crucial role in reflecting epidemiological spread. As an effect of growing international trade, intensive human mobility and inevitable menace of contagious epidemics, in-depth understanding of statistical and dynamical properties of human travel are essentially important [6]. We now assume both susceptible and infectious populations also perform random movement within their city. **We consider habitat Ω_1 and $\Omega_2 \in R^2$ as a bounded identical domain with smooth boundary $\partial\Omega_1$ and $\partial\Omega_2$ representing city 1 and city 2 respectively.** Two cities are considered to be identical. Here we also assume that β_1 and β_2 depends on the spatial location $p_1 = (x_1, y_1)$ and $p_2 = (x_2, y_2)$, is positive Hölder continuous function on Ω_1 and Ω_2 respectively. The Laplacian operator $\nabla^2 = \frac{\partial^2}{\partial x^2} + \frac{\partial^2}{\partial y^2}$, is used to describe the local Brownian motion in two-dimensional space. It can be interpreted as the non-regular and continuous movement of individuals. Incorporating these facts, equation (1)-(4) can be written in R^2 domain as

$$\frac{\partial S_1}{\partial t} = D_{S_1} \nabla^2 S_1 + f_1(S_1(p_1, t), I_1(p_1, t)) + m_1 S_2(p_2, t) - m_2 S_1(p_1, t), \quad p_1 \in \Omega_1, \quad p_2 \in \Omega_2, \quad (5)$$

$$\frac{\partial I_1}{\partial t} = D_{I_1} \nabla^2 I_1 + f_2(S_1(p_1, t), I_1(p_1, t)) + m_3 I_2(p_2, t) - m_4 I_1(p_1, t), \quad p_1 \in \Omega_1, \quad p_2 \in \Omega_2, \quad (6)$$

$$\frac{\partial S_2}{\partial t} = D_{S_2} \nabla^2 S_2 + f_3(S_2(p_2, t), I_2(p_2, t)) + m_2 S_1(p_1, t) - m_1 S_2(p_2, t), \quad p_1 \in \Omega_1, \quad p_2 \in \Omega_2, \quad (7)$$

$$\frac{\partial I_2}{\partial t} = D_{I_2} \nabla^2 I_2 + f_4(S_2(p_2, t), I_2(p_2, t)) + m_4 I_1(p_1, t) - m_3 I_2(p_2, t), \quad p_1 \in \Omega_1, \quad p_2 \in \Omega_2. \quad (8)$$

Now, consider a translation map $f : \Omega_1 \rightarrow \Omega_2$ with $p_2 = f(p_1) = p_1 + L$, L represents a fixed distance from one city to another. As per our knowledge, this situation has not been modelled yet and is an initial step for modelling movement of individuals between both inter and intra city. As all models, this model too is limited by some assumptions like that the cities are identical and people from one city move another city at exactly the same position obeying some fixed distance law. However, we hope this research work will open many paths towards modelling movement of population in any desired location within a different city. Under this map any position p_2 in city 2 can be reflected by position p_1 in city 1. Mathematically, we can write

$$\begin{aligned} S_2(p_2, t) &= \hat{S}_2(p_1, t), \quad p_1 \in \Omega_1, p_2 \in \Omega_2, \\ I_2(p_2, t) &= \hat{I}_2(p_1, t), \quad p_1 \in \Omega_1, p_2 \in \Omega_2. \end{aligned}$$

Therefore, (5)-(8) is equivalent to

$$\partial_t S_1 - D_{S_1} \nabla^2 S_1 = f_1(S_1(p_1, t), I_1(p_1, t)) + m_1 \hat{S}_2(p_1, t) - m_2 S_1(p_1, t) = g_1(S_1, I_1, \hat{S}_2), \quad p_1 \in \Omega_1, \quad (9)$$

$$\partial_t I_1 - D_{I_1} \nabla^2 I_1 = f_2(S_1(p_1, t), I_1(p_1, t)) + m_3 \hat{I}_2(p_1, t) - m_4 I_1(p_1, t) = g_2(S_1, I_1, \hat{I}_2), \quad p_1 \in \Omega_1, \quad (10)$$

$$\partial_t S_2 - D_{S_2} \nabla^2 S_2 = f_3(\hat{S}_2(p_1, t), \hat{I}_2(p_1, t)) + m_2 S_1(p_1, t) - m_1 \hat{S}_2(p_1, t) = g_3(\hat{S}_2, \hat{I}_2, S_1), \quad p_1 \in \Omega_1, \quad (11)$$

$$\partial_t I_2 - D_{I_2} \nabla^2 I_2 = f_4(\hat{S}_2(p_1, t), \hat{I}_2(p_1, t)) + m_4 I_1(p_1, t) - m_3 \hat{I}_2(p_1, t) = g_4(\hat{S}_2, \hat{I}_2, I_1) \quad p_1 \in \Omega_1. \quad (12)$$

For the sake of neat and general representation of variables we drop $\hat{\cdot}$ notation i.e. we write $\hat{S}_2 = S_2$ and $\hat{I}_2 = I_2$ we rewrite the equation (9)-(12) as follows

$$\partial_t S_1 - D_{S_1} \nabla^2 S_1 = f_1(S_1(x, t), I_1(x, t)) + m_1 S_2(x, t) - m_2 S_1(x, t) = g_1(S_1, I_1, S_2), \quad x \in \Omega, \quad (13)$$

$$\partial_t I_1 - D_{I_1} \nabla^2 I_1 = f_2(S_1(x, t), I_1(x, t)) + m_3 I_2(x, t) - m_4 I_1(x, t) = g_2(S_1, I_1, I_2), \quad x \in \Omega, \quad (14)$$

$$\partial_t S_2 - D_{S_2} \nabla^2 S_2 = f_3(S_2(x, t), I_2(x, t)) + m_2 S_1(x, t) - m_1 S_2(x, t) = g_3(S_2, I_2, S_1), \quad x \in \Omega, \quad (15)$$

$$\partial_t I_2 - D_{I_2} \nabla^2 I_2 = f_4(S_2(x, t), I_2(x, t)) + m_4 I_1(x, t) - m_3 I_2(x, t) = g_4(S_2, I_2, I_1) \quad x \in \Omega. \quad (16)$$

The system can be written compactly as,

$$\frac{\partial u}{\partial t} = D \nabla^2 u + \xi(u), \quad x \in \Omega, \quad (17)$$

where $u = (S_1, I_1, S_2, I_2)^T$, $D = (D_{S_1}, D_{I_1}, D_{S_2}, D_{I_2})^T$ and $\xi(u) = \begin{pmatrix} g_1(S_1, I_1, S_2) \\ g_2(S_1, I_1, I_2) \\ g_3(S_2, I_2, S_1) \\ g_4(S_2, I_2, I_1) \end{pmatrix}$.

The system (17) is analyzed under the initial conditions given by

$$S_{10}(x, 0) \geq 0, I_{10}(x, 0) \geq 0, S_{20}(x, 0) \geq 0, I_{20}(x, 0) \geq 0, \quad (18)$$

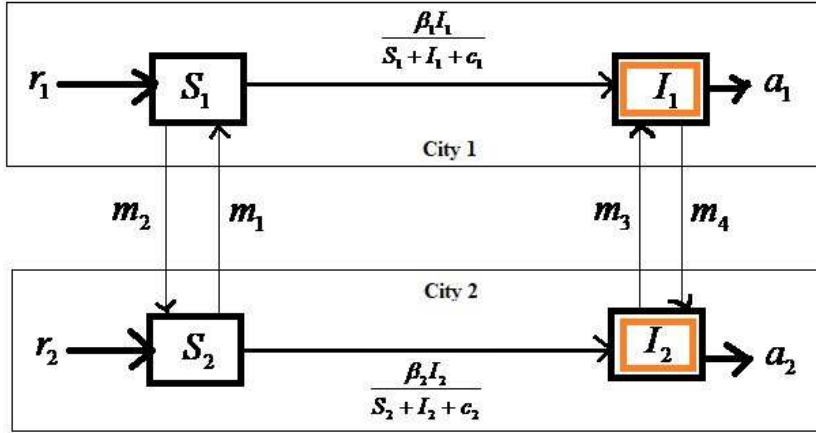


Fig. 1 Transfer diagram of the two-city model for disease transmission.

where $x \in \Omega \in \mathbb{R}^2$ and zero flux boundary conditions

$$\frac{\partial S_1}{\partial \nu} = \frac{\partial I_1}{\partial \nu} = \frac{\partial S_2}{\partial \nu} = \frac{\partial I_2}{\partial \nu} = 0. \quad (19)$$

ν represents the outward unit normal vector on the boundary $\partial\Omega$ which is assumed to be smooth. Neumann or zero-flux boundary conditions biologically implies that the domain boundary is isolated or insulated from the external environment i.e. there are no fluxes of populations through the boundary [40]. By the standard parabolic theory, (17) admits a unique nonnegative classical solution $(S_1(x, t), I_1(x, t), S_2(x, t), I_2(x, t)) \in C^{2,1}(\bar{\Omega} \times (0, \infty))$, and satisfies (17) point wisely. Moreover, from the strong maximum principle and the Hopf boundary lemma for parabolic equations [46] guarantee that $S_1(x, t), I_1(x, t), S_2(x, t), I_2(x, t) > 0$ for all $(x, t) \in \bar{\Omega} \times (0, \infty)$.

We now define two travel matrix

$$A = (a_{ij})_{2 \times 2} = \begin{pmatrix} 0 & m_2 \\ m_1 & 0 \end{pmatrix}, \quad \text{and} \quad B = (b_{ij})_{2 \times 2} = \begin{pmatrix} 0 & m_4 \\ m_3 & 0 \end{pmatrix}. \quad (20)$$

Here, a_{ij} and b_{ij} describe the mobility rate of susceptible and infected from a city i to city j respectively. We assume these matrices are irreducible. Biologically, it means individuals in city 1 can travel to city 2 directly or indirectly.

3 Dynamical behaviour of the two-city model

Before studying the stability behavior of our spatial model we give the following result to show the boundedness of system (17) which is important from ecological point of view.

3.1 Some preliminary properties of the spatial model

Proposition 1 *All non-negative solutions of model system (1)-(4) which initiate in \mathbb{R}_+^4 are uniformly bounded, with ultimate bound $(\frac{r_1}{4\eta} + 1)K_1 + (\frac{r_2}{4\eta} + 1)K_2$, where $\eta = \min(a_1, a_2)$.*

Proof We define,

$$W(t) = S_1(t) + I_1(t) + S_2(t) + I_2(t). \quad (21)$$

The time derivative of (21) along the solutions of (1)-(4) is

$$\frac{dW}{dt} = \frac{dS_1}{dt} + \frac{dI_1}{dt} + \frac{dS_2}{dt} + \frac{dI_2}{dt}, \quad (22)$$

Table 1 Parameter values of system (17) and their biological meanings. We mostly took hypothetical parameter value which are in ecological permissible range.

Variable/ Parameter	Parameter values	Description
$S_1(t)$	$S_1(0) = 1100$	Susceptible density in city 1 at time t .
$I_1(t)$	$I_1(0) = 89$	Infected density in city 1 at time t .
$S_2(t)$	$S_2(0) = 1233$	Susceptible density in city 2 at time t .
$I_2(t)$	$I_2(0) = 10$	Infected density in city 2 at time t .
r_1, r_2	1.02951, 2.23	Growth rate of susceptible in city 1 and 2 respectively.
K_1, K_2	5000, 2000	Carrying capacity of city 1 and 2 respectively.
β_1	2.15	Transmission rate of city 1.
c_1, c_2	10, 20	Constants which display a saturation effect due to the social or spacial distribution of the population and limitation of time.
β_2	0.98	Transmission rate of city 2.
a_1, a_2	0.15, 2.13	Recovery rate of the infective in city 1 and 2 respectively.
m_1	1.2	Migration rate of susceptible from city 2 to city 1.
m_2	3.2	Migration rate of susceptible from city 1 to city 2.
m_3	0.2	Migration rate of infectives from city 2 to city 1.
m_4	3.1	Migration rate of infectives from city 1 to city 2.
D_{S_1}, D_{I_1}	5, 0.01	Diffusion coefficient of susceptible and infectives of city 1 respectively.
D_{S_2}, D_{I_2}	10, 0.05	Diffusion coefficient of susceptible and infectives of city 2 respectively.

for each $\eta > 0$, the following inequality hold:

$$\frac{dW}{dt} + \eta W = r_1 S_1 \left(1 - \frac{S_1 + I_1}{K_1}\right) + r_2 S_2 \left(1 - \frac{S_2 + I_2}{K_2}\right) - (a_1 - \eta) I_1 - (a_2 - \eta) I_2 + \eta (S_1 + S_2),$$

Taking $\eta = \min(a_1, a_2)$, the above inequality satisfies

$$\frac{dW}{dt} + \eta W \leq r_1 S_1 \left(1 - \frac{S_1}{K_1}\right) + r_2 S_2 \left(1 - \frac{S_2}{K_2}\right) + \eta S_1 + \eta S_2.$$

$$\frac{dW}{dt} + \eta W \leq \left(\frac{r_1}{4} + \eta\right) K_1 + \left(\frac{r_2}{4} + \eta\right) K_2 = L. \quad (23)$$

Using comparison lemma for $t > \tilde{T} > 0$ we have

$$W(t) \leq \frac{L}{\eta} - \left(\frac{L}{\eta} - W(\tilde{T})\right) e^{-\eta(t-\tilde{T})}. \quad (24)$$

Then for $\tilde{T} = 0$ we have

$$W(t) \leq \frac{L}{\eta} - \left(\frac{L}{\eta} - W(0)\right) e^{-\eta(t)}. \quad (25)$$

For large value of t , we have $W(t) \leq \frac{L}{\eta}$ with $\eta = \min(a_1, a_2)$.

For a biologically practical system all population are required to be constrained by a bound in time by their environments. Thus, the feasible region of (1)-(4) can be chosen as $\mathcal{E} = \{(S_1, I_1, S_2, I_2) \in R_+^4 | W(t) = S_1(t) + I_1(t) + S_2(t) + I_2(t) \leq \frac{L}{\eta}\}$. It can be easily seen that \mathcal{E} is positively invariant with respect to (1)-(4). Let us denote \mathcal{E}^0 for the interior of \mathcal{E} , and $\partial\mathcal{E}$ the boundary of \mathcal{E} .

Proposition 2 All non-negative solution (S_1, I_1, S_2, I_2) of model (17) with initial condition (18), satisfies the following inequality

$$\begin{aligned} \limsup_{t \rightarrow \infty} \max_{x \in \Omega} (S_1(., t) + S_2(., t)) &\leq \max\{K, \max_{\Omega} (S_{10}(x) + S_{20}(x))\}, \\ \limsup_{t \rightarrow \infty} \max_{x \in \Omega} (I_1(., t) + I_2(., t)) &\leq \max\left(\frac{\beta K - a(c + K)}{a}, \max_{\Omega} (I_{10}(x) + I_{20}(x))\right). \end{aligned}$$

where the meaning of a, β, K can be found in proof.

Proof By virtue of (13) and (15) we have the following inequality,

$$\frac{\partial S_1}{\partial t} \leq D_{S_1} \Delta S_1 + r_1 S_1 \left(1 - \frac{S_1}{K_1}\right) + m_1 S_2 - m_2 S_1, \quad (26)$$

$$\frac{\partial S_2}{\partial t} \leq D_{S_2} \Delta S_2 + r_2 S_2 \left(1 - \frac{S_2}{K_2}\right) + m_2 S_1 - m_1 S_2. \quad (27)$$

Since the system (26)- (27) is cooperative, therefore by using comparison principle of parabolic equations [12], one can show $(S_1(x, t), S_2(x, t))$ is a subsolution of the following problem

$$\frac{d\bar{S}_1}{dt} = r_1 \bar{S}_1 \left(1 - \frac{\bar{S}_1}{K_1}\right) + m_1 \bar{S}_2 - m_2 \bar{S}_1, \quad (28)$$

$$\frac{d\bar{S}_2}{dt} = r_2 \bar{S}_2 \left(1 - \frac{\bar{S}_2}{K_2}\right) + m_2 \bar{S}_1 - m_1 \bar{S}_2. \quad (29)$$

Let $S = \bar{S}_1 + \bar{S}_2$. Adding (28) and (29) and performing straightforward computations, we get

$$\begin{aligned} \frac{d(\bar{S}_1 + \bar{S}_2)}{dt} &= r_1 \bar{S}_1 \left(1 - \frac{\bar{S}_1}{K_1}\right) + r_2 \bar{S}_2 \left(1 - \frac{\bar{S}_2}{K_2}\right), \\ \frac{dS}{dt} &\leq 2rS \left(1 - \frac{S}{K}\right), \end{aligned}$$

where $r = \max(r_1, r_2)$, and $K = \max(K_1, K_2)$. Again, using comparison principle one can show $S(t)$ is a subsolution of the following problem

$$\frac{d\bar{S}}{dt} = 2r\bar{S} \left(1 - \frac{\bar{S}}{K}\right).$$

We observe that the positive constant

$$\bar{S} = \max\{K, \max_{\bar{\Omega}}(S_{10}(x) + S_{20}(x))\}, \quad (30)$$

is the supersolution to (28)-(29). Therefore,

$$\bar{S}_1(t) + \bar{S}_2(t) \leq S(t) \leq \bar{S}(t).$$

Also, $\lim_{t \rightarrow \infty} \bar{S}(t) \leq K$. Thus, from well known comparison principle for parabolic equations, we finally have

$$S_1(x, t) + S_2(x, t) \leq \bar{S}_1(t) + \bar{S}_2(t) \leq \max\{K, \max_{\bar{\Omega}}(S_{10}(x) + S_{20}(x))\} := \bar{S}(t), \forall x \in \Omega, t \geq 0. \quad (31)$$

Hence, we have

$$S_1(x, t) + S_2(x, t) \leq K = \bar{U}_1 := \text{Sup}_{t \geq 0} \|S_1(\cdot, x) + S_2(\cdot, x)\|_{\infty}, \forall x \in \bar{\Omega},$$

This implies

$$\limsup_{t \rightarrow \infty} \max_{x \in \bar{\Omega}} (S_1(x, t) + S_2(x, t)) \leq \max\{K, \max_{\bar{\Omega}}(S_{10}(x) + S_{20}(x))\}.$$

Next, making use of (14) and (16) and putting upper bound of S_1 and S_2 we have the following inequality,

$$\frac{\partial I_1}{\partial t} \leq D_{I_1} \Delta I_1 + \frac{\beta_1 \bar{U}_1 (I_1 + I_2)}{\bar{U}_1 + (I_1 + I_2) + c_1} - a_1 I_1 + m_3 I_2 - m_4 I_1, \quad (32)$$

$$\frac{\partial I_2}{\partial t} \leq D_{I_2} \Delta I_2 + \frac{\beta_2 \bar{U}_1 (I_1 + I_2)}{\bar{U}_1 + (I_1 + I_2) + c_2} - a_2 I_2 + m_4 I_1 - m_3 I_2. \quad (33)$$

Again, since the system (32)- (33) is cooperative by using comparison principle of parabolic equations [12], one can show $(I_1(x, t), I_2(x, t)) \leq (\bar{I}_1(t), \bar{I}_2(t))$, where $(\bar{I}_1(t), \bar{I}_2(t))$ is a solution of the following differential equation

$$\frac{d\bar{I}_1}{dt} = \frac{\beta_1 \bar{U}_1 (\bar{I}_1 + \bar{I}_2)}{\bar{U}_1 + (\bar{I}_1 + \bar{I}_2) + c_1} - a_1 \bar{I}_1 + m_3 \bar{I}_2 - m_4 \bar{I}_1, \quad (34)$$

$$\frac{d\bar{I}_2}{dt} = \frac{\beta_2 \bar{U}_1 (\bar{I}_1 + \bar{I}_2)}{\bar{U}_1 + (\bar{I}_1 + \bar{I}_2) + c_2} - a_2 \bar{I}_2 + m_4 \bar{I}_1 - m_3 \bar{I}_2. \quad (35)$$

Adding (34)-(35) along with few computations and letting $I = \bar{I}_1 + \bar{I}_2$, we have the following

$$\frac{dI}{dt} \leq \left(\frac{\beta K}{K + I + c} - a \right) I,$$

where $\beta = \max(\beta_1, \beta_2)$, $a = \min(a_1, a_2)$ and $c = \min(c_1, c_2)$. Following the same analysis as above, one can show that for $t \geq 0$ we have the following inequality

$$I_1(x, t) + I_2(x, t) \leq \bar{I}_1(t) + \bar{I}_2(t) \leq \max \left(\frac{\beta K - a(c + K)}{a}, \max_{\bar{\Omega}} (I_{10}(x) + I_{20}(x)) \right) =: \bar{I}(t), \forall x \in \Omega, t \geq 0. \quad (36)$$

Hence, we have

$$I_1(x, t) + I_2(x, t) \leq \max \left(\frac{\beta K - a(c + K)}{a}, \max_{\bar{\Omega}} (I_{10}(x) + I_{20}(x)) \right) =: \bar{U}_2, \forall x \in \bar{\Omega}, \quad (37)$$

This implies

$$\limsup_{t \rightarrow \infty} \max_{x \in \bar{\Omega}} (I_1(., t) + I_2(., t)) \leq \max \left(\frac{\beta K - a(c + K)}{a}, \max_{\bar{\Omega}} (I_{10}(x) + I_{20}(x)) \right).$$

Definition 1 [7]: The spatial model (17) is said to have the persistence property if for any nonnegative initial data $(S_{10}(x), I_{10}(x), S_{20}(x), I_{20}(x))$, there exists positive constants $\epsilon_i = \epsilon_i(S_{10}, I_{10}, S_{20}, I_{20})$ for $i = 1, 2, 3, 4$, such that corresponding solution, (S_1, I_1, S_2, I_2) of model (17) satisfies,

$$\liminf_{t \rightarrow +\infty} \min_{\bar{\Omega}} S_1(x, t) \geq \epsilon_1, \liminf_{t \rightarrow +\infty} \min_{\bar{\Omega}} I_1(x, t) \geq \epsilon_2, \liminf_{t \rightarrow +\infty} \min_{\bar{\Omega}} S_2(x, t) \geq \epsilon_3, \liminf_{t \rightarrow +\infty} \min_{\bar{\Omega}} I_2(x, t) \geq \epsilon_4.$$

Proposition 3 Assume that if

$$\beta_1 > \frac{((a_1 + m_4)(c_1 + W_1))}{W_1}, \quad r_1 > \frac{\beta_1 \bar{U}_2}{(c_1 + \bar{U}_2)},$$

$$m_2 + \frac{\beta_1 \bar{U}_2}{(c_1 + \bar{U}_2)} < r_1, \quad K_1 > \frac{r_1 \bar{U}_2 (c_1 + \bar{U}_2)}{(r_1 - m_2)(c_1 + \bar{U}_2) - \beta_1 \bar{U}_2}, \quad (38)$$

$$\beta_2 > \frac{((a_2 + m_3)(c_2 + W_3))}{W_3}, \quad r_2 > \frac{\beta_2 \bar{U}_2}{(c_2 + \bar{U}_2)},$$

$$m_1 + \frac{\beta_2 \bar{U}_2}{(c_2 + \bar{U}_2)} < r_2, \quad K_2 > \frac{r_2 \bar{U}_2 (c_2 + \bar{U}_2)}{(r_2 - m_1)(c_2 + \bar{U}_2) - \beta_2 \bar{U}_2}, \quad (39)$$

(where definition of W_1 and W_3 are given in the proof) holds, than system (17) has the persistence property.

Proof From (13), we have

$$\frac{\partial S_1}{\partial t} \geq D_{S_1} \Delta S_1 + r_1 S_1 \left(1 - \frac{S_1 + I_1}{K_1} \right) - \frac{\beta_1 S_1 I_1}{S_1 + I_1 + c_1} - m_2 S_1,$$

$$\frac{\partial S_1}{\partial t} \geq D_{S_1} \Delta S_1 + r_1 S_1 \left(1 - \frac{S_1}{K_1} \right) - \frac{r_1 S_1 \bar{U}_2}{K_1} - \frac{\beta_1 S_1 \bar{U}_2}{\bar{U}_2 + c_1} - m_2 S_1,$$

$$\frac{\partial S_1}{\partial t} \geq D_{S_1} \Delta S_1 + S_1 \left(r_1 \left(1 - \frac{S_1}{K_1} \right) - \frac{r_1 S_1 \bar{U}_2}{K_1} - \frac{\beta_1 S_1 \bar{U}_2}{\bar{U}_2 + c} - m_2 \right),$$

for $t > t_1$. Since (38) holds, then for small enough $\epsilon > 0$ chosen

$$\frac{K_1}{r_1} \left(r_1 \left(1 - \frac{\bar{U}_2}{K_1} \right) - m_2 - \frac{\beta_1 \bar{U}_2}{c_1 + \bar{U}_2} \right) - \epsilon > 0. \quad (40)$$

Hence, there exists $t_2 > t_1$ such that for any $t > t_2$,

$$S_1(x, t) \geq \underline{W}_1, \quad (41)$$

where $\underline{W}_1 = \frac{K_1}{r_1} \left(r_1 \left(1 - \frac{\bar{U}_2}{K_1} \right) - m_2 - \frac{\beta_1 \bar{U}_2}{c_1 + \bar{U}_2} \right) - \epsilon$.

Now, we apply lower bound of S_1 to equation (14), and we have

$$\frac{\partial I_1}{\partial t} \geq D_I \Delta I_1 + \left(\frac{\beta_1 \underline{W}_1}{\underline{W}_1 + I_1 + c_1} - a_1 - m_4 \right) I_1. \quad (42)$$

Then there exists $t_3 > t_2$ such that for any $t > t_3$,

$$I_1(x, t) \geq \underline{W}_2, \quad (43)$$

where

$$\underline{W}_2 = -c_1 + \underline{W}_1 \left(\frac{\beta_1}{a_1 + m_4} - 1 \right) - \epsilon. \quad (44)$$

Similarly, we can find bounds for S_2 and I_2 .

$$\begin{aligned} S_2(x, t) &\geq \underline{W}_3 = \frac{K_2}{r_2} \left(r_2 \left(1 - \frac{\bar{U}_2}{K_2} \right) - m_1 - \frac{\beta_2 \bar{U}_2}{c_2 + \bar{U}_2} \right) - \epsilon, \\ I_2(x, t) &\geq \underline{W}_4 = -c_2 + \underline{W}_3 \left(\frac{\beta_2}{a_2 + m_3} - 1 \right) - \epsilon. \end{aligned} \quad (45)$$

Summarizing, we have the following

$$\begin{aligned} \liminf_{t \rightarrow \infty} \min_{\bar{\Omega}} S_1(r, t) &\geq \underline{W}_1. \\ \liminf_{t \rightarrow \infty} \min_{\bar{\Omega}} I_1(r, t) &\geq \underline{W}_2. \\ \liminf_{t \rightarrow \infty} \min_{\bar{\Omega}} S_2(r, t) &\geq \underline{W}_3. \\ \liminf_{t \rightarrow \infty} \min_{\bar{\Omega}} I_2(r, t) &\geq \underline{W}_4. \end{aligned} \quad (46)$$

Thus, the model system (17) is persistent.

3.2 Possible equilibria and their existence criteria

Our main interest in this section is the existence and uniqueness of the equilibrium. For this purpose let us first introduce some notations. For a closed linear operator $A : D(A) \subset L^2(\Omega) \rightarrow L^2(\Omega)$, where $D(A)$ is the domain of A , the spectral spread $s(A)$ of A is defined by

$$s(A) = \sup\{Re(\lambda) : \lambda \in \sigma_p(A)\},$$

where σ_p denotes the point spectrum of A .

We will first discuss equilibrium points in City 1 without any migration. There are only two equilibria for the following elliptic problem,

$$\begin{aligned} 0 &= r_1 S_1 \left(1 - \frac{S_1 + I_1}{K_1} \right) - \frac{\beta_1 S_1 I_1}{S_1 + I_1 + c_1} + D_{S_1} \nabla^2 S_1, \\ 0 &= \frac{\beta_1 S_1 I_1}{S_1 + I_1 + c_1} - a_1 I_1 + D_{I_1} \nabla^2 I_1, \end{aligned} \quad (47)$$

with boundary conditions

$$\frac{\partial S_1}{\partial \nu} = \frac{\partial I_1}{\partial \nu} = 0, x \in \partial\Omega.$$

The system has,

1. A disease free equilibrium (DFE) is a time independent solution of the form $E_{10} = (S_{10}^0, 0)$, where $S_{10}^0 > 0$ for $x \in \Omega$. It is obvious that $(S_{10}^0, 0)$ is a disease free equilibrium if and only if S_{10}^0 is a positive solution of the equation,

$$D_{S_1} \nabla^2 S_1 + S_1 r_1 \left(1 - \frac{S_1}{K_1}\right) = 0, x \in \Omega. \quad (48)$$

Now, we state the following proposition [49]

Proposition 4 Equation (48) has a positive solution S_{10}^0 if and only if $s(D_{S_1} \nabla^2 + r_1) > 0$. Moreover, the positive solution S_{10}^0 is unique and it is strictly positive on Ω .

2. An endemic equilibrium $E_{10}^*(S_{10}^*, I_{10}^*)$ exists iff there is a positive solution to the (47).

For more generality we investigate the existence of endemic equilibrium when $\beta(x), a_1(x), r_1(x)$ are positive Hölder continuous functions on Ω . Before the main result, we state a useful lemma [33],

Lemma 1 Let Ω be a bounded Lipschitz domain in R^n . Let Λ be a non-negative constant and suppose that $z \in W^{1,2}(\Omega)$ is a non-negative weak solution of the inequalities

$$0 \leq -\nabla^2 z + \Lambda z \quad \text{in } \Omega, \quad \frac{\partial z}{\partial \nu} \leq 0 \quad \text{on } \partial\Omega.$$

Then, for any $q \in [1, n/(n-2)]$, there exists a positive constant C_0 , depending on q, Λ and Ω , such that $\|z\|_q \leq C_0 \inf z$.

Proposition 5 Problem (47) admits at least one positive solution.

Proof The proof uses the approach given by [54]; [29]; [30]; [43]. But for the reader convenience we summarize the steps of the proof given in Appendix A.

Now, we give two simple observations which give the existence of equilibrium points for the other cities and hence give us an idea about the existence of equilibrium for the entire network.

Remark 1. Suppose that system (17) is at an equilibrium $E_0 = (S_1^0, 0, S_2^0, 0)$, and given city 1 is at disease free equilibrium, E_{10} . Then city 2 that can be accessed from city 1 is also at the DFE. In particular, if outgoing matrices A and B are irreducible, then both cities are at the DFE. Indeed for showing this, suppose the city 1 is at the DFE, i.e., $I_1 = 0$. Then from eqn (14) we have

$$\frac{\partial I_1}{\partial t} = m_3 I_2.$$

As the city 1 is in disease free equilibrium, $\frac{\partial I_1}{\partial t} = 0$, now since $m_3 > 0$ it follows that $I_2 = 0$. This implies that the entire system is at disease free equilibrium, E_0 .

Remark 2. Suppose that system (17) is at an equilibrium $E^* = (S_1^*, I_1^*, S_2^*, I_2^*)$, and that the disease is endemic in city 1. Then the disease is also endemic in city 2 that can be accessed from city 1. In particular, if the outgoing matrices A and B are irreducible, then the disease is endemic in both cities. Indeed for showing this, suppose that the disease is endemic in city 1, i.e., $I_1 > 0$. We will prove this result by contradiction. Suppose that $I_2 = 0$. Since the system is at equilibrium, from (16) we have

$$0 = \frac{\partial I_2}{\partial t} = m_4 I_1.$$

Again since $m_4 > 0$, it follows $I_1 = 0$, which is a contradiction. Therefore $I_2 > 0$ if the disease is endemic in city 1.

Similar results were obtained for the ODE multi-city epidemic model [3]. These results can be extended for n cities in the similar way. Moreover these results give an idea that if the cities are connected and have access to each other then either both cities will be disease-free or both will be in disease endemic situations. We have illustrated this result numerically in section 5.

3.3 Calculation of Basic Reproduction Number

The basic reproduction number, R_0 is interpreted as the expected number of new cases generated by a single infected host in a completely susceptible population [11]. This number is very useful because it assists to figure out whether infectious disease will spread through the population or will die out. Following the steps in [52] we first calculate the basic reproduction number for system (1)-(4). For the epidemic (1)-(4), we define:

$$F = \begin{pmatrix} \frac{\beta_1 S_1^0}{S_1^0 + c_1} & 0 \\ 0 & \frac{\beta_2 S_2^0}{S_2^0 + c_2} \end{pmatrix}, V = \begin{pmatrix} m_4 + a_1 & -m_3 \\ -m_4 & m_3 + a_2 \end{pmatrix}. \quad (49)$$

The basic reproduction number can be calculated by finding the spectral radius of the next generation matrix FV^{-1} .

$$R_0^{ODE} = \max\{R_{01}^{ODE}, R_{02}^{ODE}\}, \quad (50)$$

where R_{0j}^{ODE} ($j = 1, 2$) is the basic reproduction number of each city given by

$$R_{01}^{ODE} = \frac{\beta_1(a_2 + m_3)S_1^0}{(a_1(a_2 + m_3) + a_2m_4)(c_1 + S_1^0)}, R_{02}^{ODE} = \frac{\beta_2(a_1 + m_4)S_2^0}{(a_1(a_2 + m_3) + a_2m_4)(c_2 + S_2^0)}.$$

Now, in order to define the basic reproduction number for model (17), we use the approach given by [58]; [45]. We assume that the state variables are near the disease-free steady state, E_0 . Let the distribution of initial infection is represented by $\phi(x)$. Under the affect of mortality, mobility and transfer of individuals in infected compartments, the distribution of those infective members as time evolves becomes $T(t)\phi(x)$. Thus, the distribution of new infection at time t is $F(x)T(t)\phi(x)$. Subsequently, the distribution of total new infection is

$$\int_0^\infty F(x)T(t)\phi(x)dt. \quad (51)$$

Define

$$L(\phi)(x) := \int_0^\infty F(x)T(t)\phi dt = F(x) \int_0^\infty T(t)\phi dt.$$

L is a positive continuous operator which maps the initial infection distribution of the total infective members produced during the infection period. Following [58]; [36] we define spectral radius of L as the basic reproduction number

$$R_0^{HPDE} := r(L) \quad (R_0^{HPDE} \text{ represents basic reproduction number in heterogeneous environment}) \quad (52)$$

for model (17).

Now, we define the basic reproduction number R_{01}^{HPDE} for the system of isolated city 1. We linearize the system around the DFE $E_{10} = (S_{10}^0, 0)$ and obtain the following equation

$$\begin{aligned} \frac{\partial I_1}{\partial t} &= D_{I_1} \nabla^2 I_1 + \left(\frac{\beta_1 S_{10}^0}{S_{10}^0 + c_1} - a_1 \right) I_1, \\ \frac{\partial I_1}{\partial \nu} &= 0. \end{aligned} \quad (53)$$

By substituting $I_1(x, t) = e^{-\lambda t} \xi(x)$, $\lambda \in \mathbb{R}$ into the equation and dividing both sides by $e^{-\lambda t}$, we obtain the following linear eigenvalue problem

$$\begin{aligned} D_{I_1} \nabla^2 \xi + \left(\frac{\beta_1 S_{10}^0}{S_{10}^0 + c_1} - a_1 \right) \xi + \lambda \xi &= 0, \\ \frac{\partial \xi}{\partial \nu} &= 0. \end{aligned} \quad (54)$$

By the Krein-Rutman Theorem [21], if (λ, ξ) is a solution of (54) with $\xi \neq 0$ on Ω then λ is real. Moreover, there exists a least eigenvalue λ^* , with its corresponding eigenfunction ξ^* positive on Ω .

Also, there is no other eigenvalue λ that has an eigenfunction ξ which is positive everywhere. Notice that (λ^*, ξ^*) satisfies

$$D_{I_1} \nabla^2 \xi^* + \left(\frac{\beta_1(x) S_{10}^0}{S_{10}^0 + c_1} - a_1 \right) \xi^* + \lambda^* \xi^* = 0.$$

Following [1], λ^* is given by the variational characterization as:

$$\lambda^* = \inf \left\{ \int_{\Omega} D_{I_1} |\nabla \phi(x)|^2 + \left(a_1 - \frac{\beta_1(x) S_{10}^0}{S_{10}^0 + c_1} \right) \phi^2(x) : \phi \in W^{1,2}(\Omega) \text{ and } \int_{\Omega} \phi dx = 1 \right\},$$

$$R_{01}^{HPDE} = \sup \left\{ \frac{\int \frac{\beta_1(x) S_{10}^0}{S_{10}^0 + c_1} \phi^2(x) dx}{\int [D_{I_1} |\nabla \phi(x)|^2 + a_1 \phi^2(x)] dx} : \phi \in W^{1,2}(\Omega) \right\}. \quad (55)$$

Similarly for city 2,

$$R_{02}^{HPDE} = \sup \left\{ \frac{\int \frac{\beta_2(x) S_{20}^0}{S_{20}^0 + c_2} \phi^2(x) dx}{\int [D_{I_2} |\nabla \phi(x)|^2 + a_2 \phi^2(x)] dx} : \phi \in W^{1,2}(\Omega) \right\}. \quad (56)$$

The definition of R_0^{HPDE} for (17) is closely related to the stability of DFE, $E_0 = (S_1^0, 0, S_2^0, 0)$. Linearizing the model around E_0 , the stability of E_0 can be decided by the sign of the principal eigenvalue of the problem:

$$\begin{aligned} \mu \phi_1 &= D_{I_1} \nabla^2 \phi_1 + \left(\frac{\beta_1(x) S_1}{S_1 + c_1} - (m_4 + a_1) \right) \phi_1 + m_3 \phi_2, \quad x \in \Omega, \\ \mu \phi_2 &= D_{I_2} \nabla^2 \phi_2 + m_4 \phi_1 + \left(\frac{\beta_2(x) S_2}{S_2 + c_2} - (m_3 + a_2) \right) \phi_2, \quad x \in \Omega, \\ \frac{\partial \phi_1}{\partial \nu} &= \frac{\partial \phi_2}{\partial \nu} = 0, \quad x \in \partial \Omega. \end{aligned} \quad (57)$$

Since the system is cooperative, (57) has a principal eigenvalue μ_0 associated with a positive eigenvector [24].

Following [37], [58], [53], the basic reproduction number R_0^{HPDE} for (17) is defined as the spectral radius $r(-FO^{-1})$, where $O : D(O) \subset C(\bar{\Omega}; R^2) \rightarrow C(\bar{\Omega}; R^2)$ is a linear operator $O = \begin{pmatrix} D_{I_1} \nabla^2 & 0 \\ 0 & D_{I_2} \nabla^2 \end{pmatrix} - V$. F and V are as defined in (49).

$$D(O) = (\phi_1, \phi_2) \in \cap_{p \geq 1} W^{2,p}(\Omega; R) : \frac{\partial \phi_1}{\partial \nu} = \frac{\partial \phi_2}{\partial \nu} = 0, \text{ on } \partial \Omega \text{ and } O(\phi_1, \phi_2) \in C(\bar{\Omega}; R^2).$$

However, when the infection coefficients β_1 and β_2 are spatially independent, the basic reproduction number admits the same value as its ODE counterpart [11]. We state the following result from [58]:

Theorem 1 *If each D_{S_1} , D_{I_1} , D_{S_2} and D_{I_2} is a positive constant and $F(x) = F$ and $V(x) = V$ are independent of $x \in \Omega$, then basic reproduction number for homogeneous environment $R_0^{HPDE} = r(FV^{-1}) = R_0^{ODE}$.*

Proof See [58] for the proof.

Section 5 gives numerical evidence for these analytical results.

4 Global Stability Analysis

In this section, we deduce sufficient conditions under which the disease free and endemic equilibrium globally asymptotically stable in a homogeneous environment. Graph theoretical approaches developed by [32] are utilized in our proof. Before starting, we recall some preliminaries from graph theory.

Consider a weighted *directed* graph or *digraph* $G = (W, E)$ containing a set $W = \{1, 2, 3, \dots, n\}$ of vertices and a set E of arcs (i, j) leading from source vertex i to destination vertex j and each arc (j, i) is assigned a positive weight m_{ij} . The weight matrix of weighted digraph is given by $M = (m_{ij})_{n \times n}$ whose entry m_{ij} equals the weight of arc (j, i) if it exists, and 0 otherwise. A weighted digraph (G, M)

is strongly connected if and only if the weight matrix M is irreducible. The Laplacian matrix of (G, M)

$$\text{is defined as } L = \begin{pmatrix} \sum_{k \neq 1} m_{1k} & -m_{12} & \dots & -m_{1n} \\ -m_{21} & \sum_{k \neq 2} m_{2k} & \dots & -m_{2n} \\ \vdots & \vdots & \vdots & \vdots \\ -m_{n1} & -m_{n2} & \dots & \sum_{k \neq n} m_{nk} \end{pmatrix},$$

Let C_i denote the cofactor of the i^{th} diagonal element of L . The result which will be used in our proofs are given as follows [20]:

Proposition 6 Assume $n \geq 2$. Then

$$C_i = \sum_{T \in T_i} W(T), i = 1, 2, 3, \dots, n. \quad (58)$$

where T_i is the set of all spanning trees T of (G, M) that are rooted at vertex i , and $W(T)$ is the weight of T . In particular, if (G, M) is strongly connected, then $C_i > 0$ for $1 \leq i \leq n$.

Theorem 2 Assume $n \geq 2$. Let C_i be given in the above proposition. Then the following identity holds:

$$\sum_{i,j=1}^n C_i m_{ij} G_i(x_i) = \sum_{i,j=1}^n C_i m_{ij} G_j(x_j), \quad (59)$$

where $G_i(x_i)$, $1 \leq i \leq n$, are arbitrary functions.

Proposition 7 Assume $R_0^{ODE} \leq 1$. Suppose that infective travel matrix $B = (b_{ij})$ is irreducible. Then the disease-free equilibrium E_0 is globally asymptotically stable.

Proof Suppose $B = (b_{ij})$ is irreducible (see (20)). Let F and V be given as in (49). We observe that V is a non-singular M-matrix since all the off-diagonal entries of V are non-positive and the sum of the entries of each of its columns are positive. Since B is irreducible, then $V^{-1} > 0$ is also irreducible. By Perron-Frobenius Theorem [4], non-negative irreducible matrix $V^{-1}F$ has a positive left eigenvector (w_1, w_2) corresponding to eigenvalue $\rho(V^{-1}F)$.

$$(w_1, w_2)F^{-1}V = R_0^{ODE}(w_1, w_2) \quad (60)$$

and thus

$$\frac{1}{R_0^{ODE}}(w_1, w_2) = (w_1, w_2)F^{-1}V \quad (61)$$

Let $d_i = \frac{w_i}{\beta_i S_i^0} > 0$, $i = 1, 2$ and $I = (I_1, I_2)^T$. Set

$$L_1 = d_1 I_1 + d_2 I_2. \quad (62)$$

Differentiating L_1 along solutions of system (1)-(4), we obtain

$$\begin{aligned} L_1' &= d_1 \left(\frac{\beta_1 S_1 I_1}{S_1 + I_1 + c_1} - a_1 I_1 - m_4 I_1 + m_3 I_2 \right) + d_2 \left(\frac{\beta_2 S_2 I_2}{S_2 + I_2 + c_2} - a_2 I_2 + m_4 I_1 - m_3 I_2 \right), \\ &\leq d_1 \left(\frac{\beta_1 S_1^0 I_1}{S_1^0 + c_1} - (a_1 + m_4) I_1 + m_3 I_2 \right) + d_2 \left(\frac{\beta_2 S_2^0 I_2}{S_2^0 + c_2} - (a_2 + m_3) I_2 + m_4 I_1 \right), \\ &= \left(\frac{w_1}{\beta_1 S_1^0 / (S_1^0 + c_1)}, \frac{w_2}{\beta_2 S_2^0 / (S_2^0 + c_2)} \right) (F - V)I, \\ &= (w_1, w_2)(1 - F^{-1}V)I, \\ &= (w_1, w_2) \left(1 - \frac{1}{R_0^{ODE}} \right) I \leq 0, \end{aligned}$$

Therefore, L_1 is a Lyapunov function for system (1)-(4). Since $d_i > 0$ for $i = 1, 2$, $L_1' = 0$ implies that either $S_i = S_i^0$ or $I_i = 0$ for any $1 \leq i \leq 2$. When $S_i = S_i^0$, we have

$$0 = (S_i^0)' = r_i S_i^0 \left(1 - \frac{S_i^0 + I_i}{K_i} \right) - \frac{\beta_i S_i^0 I_i}{S_i^0 + I_i + c_i} \mp m_1 S_1^0 \pm m_2 S_2^0.$$

Comparing these equations with

$$0 = r_i S_i \left(1 - \frac{S_i}{K_i}\right) \mp m_1 S_1 \pm m_2 S_2.$$

we have $I_i = 0$. Thus, we showed that $L'_1 = 0$ implies $I_1 = I_2 = 0$. It can be easily verified that the only invariant subset of the set $\{(S_1, I_1, S_2, I_2) \in |I_1, I_2 = 0\}$ is the singleton E_0 . Therefore, by LaSalle Invariance Principle[25], E_0 is globally asymptotically stable in \mathcal{E}^0 .

Now, we establish the global stability of DFE, E_0 for a homogeneous spatial model system (13)-(16). For this, we select a Lyapunov function as:

$$\mathcal{V}_1(t) = \int \int_{\Omega} L_1(I_1, I_2) dA, \quad (63)$$

where $L_1(I_1, I_2)$ is given as in (62).

$$\begin{aligned} \frac{d\mathcal{V}_1}{dt} &= \int \int_{\Omega} \left[\frac{\partial L_1}{\partial I_1} \frac{\partial I_1}{\partial t} + \frac{\partial L_1}{\partial I_2} \frac{\partial I_2}{\partial t} \right] dA, \\ &= \int \int_{\Omega} \frac{dL_1}{dt} dA + \int \int_{\Omega} \left(D_{I_1} \frac{\partial L_1}{\partial I_1} \nabla^2 I_1 + D_{I_2} \frac{\partial L_1}{\partial I_2} \nabla^2 I_2 \right) dA, \\ &= T_1 + T_2, \end{aligned}$$

where $T_1 = \int \int_{\Omega} \frac{dL_1}{dt} dA$ and $T_2 = \int \int_{\Omega} \left(D_{I_1} \frac{\partial L_1}{\partial I_1} \nabla^2 I_1 + D_{I_2} \frac{\partial L_1}{\partial I_2} \nabla^2 I_2 \right) dA$. We now consider T_2 and determine the sign of each term. We utilize the formula known as Green's first identity in the plane

$$\begin{aligned} \int \int_{\Omega} F \nabla^2 G dA &= \int_{\Omega} F \frac{\partial G}{\partial \nu} dS - \int \int_{\Omega} (\nabla F \cdot \nabla G) dA, \\ \int \int_{\Omega} \frac{\partial L_1}{\partial I_1} \nabla^2 I_1 dA &= \int_{\Omega} \frac{\partial L_1}{\partial I_1} \frac{\partial I_1}{\partial \nu} dS - \int \int_{\Omega} \left[\nabla \left(\frac{\partial L_1}{\partial I_1} \right) \cdot \nabla I_1 \right] dA, \\ &= - \int \int_{\Omega} \left[\nabla \left(\frac{\partial L_1}{\partial I_1} \right) \cdot \nabla I_1 \right] dA. \end{aligned} \quad (64)$$

Now,

$$\nabla \left(\frac{\partial L_1}{\partial I_1} \right) = \frac{\partial^2 L_1}{\partial I_1^2} \frac{\partial I_1}{\partial x} \hat{i} + \frac{\partial^2 L_1}{\partial I_1^2} \frac{\partial I_1}{\partial y} \hat{j}.$$

Hence,

$$\int \int_{\Omega} \frac{\partial L_1}{\partial I_1} \nabla^2 I_1 dA = - \int \int_{\Omega} \frac{\partial^2 L_1}{\partial I_1^2} \left[\left(\frac{\partial I_1}{\partial x} \right)^2 + \left(\frac{\partial I_1}{\partial y} \right)^2 \right] dA \leq 0.$$

Similarly,

$$\int \int_{\Omega} \frac{\partial L_1}{\partial I_2} \nabla^2 I_2 dA = - \int \int_{\Omega} \frac{\partial^2 L_1}{\partial I_2^2} \left[\left(\frac{\partial I_2}{\partial x} \right)^2 + \left(\frac{\partial I_2}{\partial y} \right)^2 \right] dA \leq 0.$$

The above analysis shows that if $T_1 \leq 0$, then $\frac{d\mathcal{V}_1(t)}{dt} \leq 0$. This implies that E_0 is globally asymptotically stable in presence of diffusion if E_0 is globally asymptotically stable in the absence of diffusion.

Proposition 8 Assume that $R_0^{ODE} > 1$ and suppose that the following assumptions are satisfied for all $1 \leq i, j \leq 2$

1. A, B are irreducible.
2. There exists $\lambda > 0$ such that $a_{ij}^* S_j^* = \lambda b_{ij} I_j^*$.
3. $S_i - \frac{(S_i + I_i)}{K_i} (S_i - S_i^*) < 0, S_i \neq S_i^*$.
4. $S_i^* (I_i - I_i^*) - I_i^* (S_i - S_i^*) < 0, S_i \neq S_i^*, I_i \neq I_i^*$.

Then there exists a unique equilibrium E^* which is globally asymptotically stable.

Proof We prove the result when all assumptions are satisfied. For city 1 set

$$\mathcal{L}_1(S_1, I_1) = S_1 - S_1^* - S_1^* \ln \frac{S_1}{S_1^*} + I_1 - I_1^* - I_1^* \ln \frac{I_1}{I_1^*}. \quad (65)$$

From equilibrium equation, we obtain

$$\begin{aligned} r_1 S_1^* - m_2 S_1^* &= r_1 S_1^* \left(\frac{S_1^* + I_1^*}{K_1} \right) + \frac{\beta_1 S_1^* I_1^*}{S_1^* + I_1^* + c_1} - m_1 S_2^*, \\ a_1 I_1^* + m_4 I_1^* &= \frac{\beta_1 S_1^* I_1^*}{S_1^* + I_1^* + c_1} + m_3 I_2^*. \end{aligned}$$

Note that $1 - x + \ln x \leq 0$ for $x > 0$ and equality holds if and only if $x = 1$. Differentiating \mathcal{L}_1 along the solution of system (1)-(4), we obtain

$$\begin{aligned} \mathcal{L}'_1 &= r_1 S_1 - r_1 S_1 \left(\frac{S_1 + I_1}{K_1} \right) - \frac{\beta_1 S_1 I_1}{S_1 + I_1 + c_1} + m_1 S_2 - m_2 S_1 \\ &+ S_1^* \left(r_1 \left(\frac{S_1 + I_1}{K_1} \right) + \frac{\beta_1 I_1}{S_1 + I_1 + c_1} - \frac{m_1 S_2}{S_1} \right) - (r_1 S_1^* - m_2 S_1^*) \\ &+ \left(\frac{\beta_1 S_1 I_1}{S_1 + I_1 + c_1} - a_1 I_1 + m_3 I_2 - m_4 I_1 \right) - I_1^* \left(\frac{\beta_1 S_1}{S_1 + I_1 + c_1} - a_1 + \frac{m_3 I_2}{I_1} - m_4 \right), \\ &\leq r_1 S_1 - r_1 S_1 \left(\frac{S_1 + I_1}{K_1} \right) + m_1 S_2 + S_1^* \left(r_1 \left(\frac{S_1 + I_1}{K_1} \right) + \frac{\beta_1 I_1}{S_1 + I_1 + c_1} - \frac{m_1 S_2}{S_1} \right) \\ &- (r_1 S_1^* \left(\frac{S_1^* + I_1^*}{K_1} \right) + \frac{\beta_1 S_1^* I_1^*}{S_1^* + I_1^* + c_1} - m_1 S_2^*) \\ &+ (m_3 I_2) - I_1^* \left(\frac{\beta_1 S_1}{S_1 + I_1 + c_1} + \frac{m_3 I_2}{I_1} \right) + \left(\frac{\beta_1 S_1^* I_1^*}{S_1^* + I_1^* + c_1} + m_3 I_2^* \right), \\ &\leq r_1 \left(S_1 - \frac{(S_1 + I_1)}{K_1} (S_1 - S_1^*) \right) + \frac{\beta_1}{S_1 + I_1 + c_1} [S_1^* (I_1 - I_1^*) - I_1^* (S_1 - S_1^*)] \\ &+ m_1 S_2^* \left(1 - \frac{S_1^* S_2}{S_2^* S_1} + \ln \frac{S_1^* S_2}{S_2^* S_1} \right) + m_1 S_2^* \left(\frac{S_2}{S_2^*} + \ln \frac{S_2^*}{S_2} - \frac{S_1}{S_1^*} - \ln \frac{S_1^*}{S_1} \right) \\ &+ m_3 I_2^* \left(1 - \frac{I_2 I_1^*}{I_2^* I_1} + \ln \frac{I_2 I_1^*}{I_2^* I_1} \right) + m_3 I_2^* \left(\frac{I_2}{I_2^*} + \ln \frac{I_2^*}{I_2} - \frac{I_1}{I_1^*} - \ln \frac{I_1^*}{I_1} \right), \\ &\leq m_1 S_2^* \left(\frac{S_2}{S_2^*} + \ln \frac{S_2^*}{S_2} - \frac{S_1}{S_1^*} - \ln \frac{S_1^*}{S_1} \right) + m_3 I_2^* \left(\frac{I_2}{I_2^*} + \ln \frac{I_2^*}{I_2} - \frac{I_1}{I_1^*} - \ln \frac{I_1^*}{I_1} \right), \\ &\leq m_3 I_2^* \left[\left(\lambda \frac{S_2}{S_2^*} + \lambda \ln \frac{S_2^*}{S_2} + \frac{I_2}{I_2^*} + \ln \frac{I_2^*}{I_2} \right) - \left(\lambda \frac{S_1}{S_1^*} + \lambda \ln \frac{S_1^*}{S_1} + \frac{I_1}{I_1^*} + \ln \frac{I_1^*}{I_1} \right) \right], \\ &= m_3 I_2^* [G_2(S_2, I_2) - G_1(S_1, I_1)], \\ &= b_{21} I_2^* [G_2(S_2, I_2) - G_1(S_1, I_1)], \end{aligned}$$

where $G_i(S_i, I_i) = \lambda \frac{S_i}{S_i^*} + \lambda \ln \frac{S_i^*}{S_i} + \lambda \frac{I_i}{I_i^*} + \lambda \ln \frac{I_i^*}{I_i}$, $i = 1, 2$.

Similarly, if we consider $\mathcal{L}_2(S_2, I_2) = S_2 - S_2^* - S_2^* \ln \frac{S_2}{S_2^*} + I_2 - I_2^* - I_2^* \ln \frac{I_2}{I_2^*}$ we have $\mathcal{L}'_2 \leq m_4 I_1^* [G_1(S_1, I_1) - G_2(S_2, I_2)] = b_{12} I_1^* [G_1(S_1, I_1) - G_2(S_2, I_2)]$. Consider a weight matrix $M = (m_{ij})$ with entry $m_{ij} = b_{ij} I_i$ and denote the corresponding weighted digraph as (G, M) . Let $C_i = \sum_{T \in \mathcal{T}_i} W(T) \geq 0$ be as given in proposition 6 with (G, M) . Then, by Theorem 2, the following identity holds

$$\sum_{i=1}^2 C_i \sum_{j=1}^2 b_{ij} I_i^* [G_i(S_i, I_i) - G_j(S_j, I_j)] = 0. \quad (66)$$

Set

$$\mathcal{L}_3(S_1, I_1, S_2, I_2) = \sum_{i=1}^2 C_i \mathcal{L}_i(S_i, I_i). \quad (67)$$

Differentiating (67) and using (66),

$$\mathcal{L}'_3 = \sum_{i=1}^2 C_i \mathcal{L}'_i \leq \sum_{i=1}^2 C_i \sum_{j=1}^2 b_{ij} I_i^* [G_i(S_i, I_i) - G_j(S_j, I_j)] = 0, \quad (68)$$

for all $(S_1, I_1, S_2, I_2) \in \mathcal{E}^0$. Therefore, \mathcal{L}_3 is a Lyapunov function for the system (1)-(4). To prove E^* is globally asymptotically stable, we need to examine the largest compact invariant set. Since B is irreducible, we know that $C_i > 0$ for $i = 1, 2$ and thus $\mathcal{L}'_3 = 0$ implies that $S_i = S_i^*$, and $I_1 = I_1^*$ for $i = 1, 2$. Therefore, the only compact invariant subset of the set where $\mathcal{L}'_3 = 0$ is the singleton E^* . Therefore, by LaSalle Invariance Principle, E^* is globally asymptotically stable in the interior of \mathcal{E}^0 .

Now, we are in position to prove the global stability of E^* for spatial model system (13)-(16). Next, we choose a Lyapunov function as

$$\mathcal{V}_2(t) = \int \int_{\Omega} \mathcal{L}_3(S_1, I_1, S_2, I_2) dA, \quad (69)$$

where $\mathcal{L}_3(S_1, I_1, S_2, I_2)$ is given as in (67). Then,

$$\begin{aligned} \frac{d\mathcal{V}_2}{dt} &= \int \int_{\Omega} \left[\frac{\partial \mathcal{L}_3}{\partial S_1} \frac{\partial S_1}{\partial t} + \frac{\partial \mathcal{L}_3}{\partial I_1} \frac{\partial I_1}{\partial t} + \frac{\partial \mathcal{L}_3}{\partial S_2} \frac{\partial S_2}{\partial t} + \frac{\partial \mathcal{L}_3}{\partial I_2} \frac{\partial I_2}{\partial t} \right] dA, \\ &= \int \int_{\Omega} \frac{d\mathcal{L}_3}{dt} dA + \int \int_{\Omega} \left(D_{S_1} \frac{\partial \mathcal{L}_3}{\partial S_1} \nabla^2 S_1 + D_{I_1} \frac{\partial \mathcal{L}_3}{\partial I_1} \nabla^2 I_1 + D_{S_2} \frac{\partial \mathcal{L}_3}{\partial S_2} \nabla^2 S_2 + D_{I_2} \frac{\partial \mathcal{L}_3}{\partial I_2} \nabla^2 I_2 \right) dA, \\ &= U_1 + U_2, \end{aligned}$$

where $U_1 = \int \int_{\Omega} \frac{d\mathcal{L}_3}{dt} dA$ and $U_2 = \int \int_{\Omega} \left(D_{S_1} \frac{\partial \mathcal{L}_3}{\partial S_1} \nabla^2 S_1 + D_{I_1} \frac{\partial \mathcal{L}_3}{\partial I_1} \nabla^2 I_1 + D_{S_2} \frac{\partial \mathcal{L}_3}{\partial S_2} \nabla^2 S_2 + D_{I_2} \frac{\partial \mathcal{L}_3}{\partial I_2} \nabla^2 I_2 \right) dA$.

$$\begin{aligned} \int \int_{\Omega} F \nabla^2 G dA &= \int_{\Omega} F \frac{\partial G}{\partial n} dS - \int \int_{\Omega} (\nabla F \cdot \nabla G) dA, \\ \int \int_{\Omega} \frac{\partial \mathcal{L}_3}{\partial S_1} \nabla^2 S_1 dA &= \int_{\Omega} \frac{\partial \mathcal{L}_3}{\partial S_1} \frac{\partial S_1}{\partial n} dS - \int \int_{\Omega} \left[\nabla \left(\frac{\partial \mathcal{L}_3}{\partial S_1} \right) \cdot \nabla S_1 \right] dA, \\ &= - \int \int_{\Omega} \left[\nabla \left(\frac{\partial \mathcal{L}_3}{\partial S_1} \right) \cdot \nabla S_1 \right] dA. \end{aligned} \quad (70)$$

Now,

$$\nabla \left(\frac{\partial \mathcal{L}_3}{\partial S_1} \right) = \frac{\partial^2 \mathcal{L}_3}{\partial S_1^2} \frac{\partial S_1}{\partial x} \hat{i} + \frac{\partial^2 \mathcal{L}_3}{\partial S_1^2} \frac{\partial S_1}{\partial y} \hat{j}, \quad (71)$$

Hence,

$$\int \int_{\Omega} \frac{\partial \mathcal{L}_3}{\partial S_1} \nabla^2 S_1 dA = - \int \int_{\Omega} \frac{\partial^2 \mathcal{L}_3}{\partial S_1^2} \left[\left(\frac{\partial S_1}{\partial x} \right)^2 + \left(\frac{\partial S_1}{\partial y} \right)^2 \right] dA \leq 0. \quad (72)$$

Similarly,

$$\begin{aligned} \int \int_{\Omega} \frac{\partial \mathcal{L}_3}{\partial I_1} \nabla^2 I_1 dA &= - \int \int_{\Omega} \frac{\partial^2 \mathcal{L}_3}{\partial I_1^2} \left[\left(\frac{\partial I_1}{\partial x} \right)^2 + \left(\frac{\partial I_1}{\partial y} \right)^2 \right] dA \leq 0, \\ \int \int_{\Omega} \frac{\partial \mathcal{L}_3}{\partial S_2} \nabla^2 S_2 dA &= - \int \int_{\Omega} \frac{\partial^2 \mathcal{L}_3}{\partial S_2^2} \left[\left(\frac{\partial S_2}{\partial x} \right)^2 + \left(\frac{\partial S_2}{\partial y} \right)^2 \right] dA \leq 0, \\ \int \int_{\Omega} \frac{\partial \mathcal{L}_3}{\partial I_2} \nabla^2 I_2 dA &= - \int \int_{\Omega} \frac{\partial^2 \mathcal{L}_3}{\partial I_2^2} \left[\left(\frac{\partial I_2}{\partial x} \right)^2 + \left(\frac{\partial I_2}{\partial y} \right)^2 \right] dA \leq 0 \end{aligned} \quad (73)$$

The above analysis indicates that if $U_1 \leq 0$, then $\frac{d\mathcal{V}_2(t)}{dt} \leq 0$. Thus, we have the following consequence: if E^* is globally asymptotically stable in the absence of diffusion, then E^* will remain globally asymptotically stable in the presence of diffusion.

The same procedure will work for homogeneous coupled reaction-diffusion system with n nodes or cities and any topology or connections.

5 Numerical Simulation For Two Cities

The global dynamical behaviour of two-city model in the interior of R_4^+ is investigated numerically. The values of the parameters are hypothetical but are chosen carefully on the basis of the ranges reported in Jorgensen (1979) [18] and are ecologically permissible parameter values. The ODEs (1)-(4) were integrated using Runge-Kutta method and for spatial model we employ explicit standard five-point approximation programmed in the MATLAB R2017a software environment.

5.1 Numerical simulation for non-spatial model and effect of mobility

For the parameter values $m_1 = 1.2, m_2 = 0.2, a_1 = 0.15, m_3 = 0.2, m_4 = 0.1, a_2 = 0.13$ and other parameters as given in Table 1 we obtain positive equilibrium point as $E^* = (48.9651, 642.9726, 52.3128, 321.6942)$, which is globally asymptotically stable (c.f. Fig. 2(a)). If we change the parameter $m_4 = 3.1$ we observe that the dynamics changes from stable focus to limit cycle (c.f. Fig. 2(b)). These figures suggest that change in migration rate can induce bifurcation.

We have used the MATLAB `matcont` toolbox for plotting equilibrium manifolds of E^* and are presented in Fig. 3(a) and 3(b). These diagrams are generated by taking m_4 and m_1 as a bifurcation parameter. In Fig. 3(a), variations of the infective I_1 and I_2 populations are given as functions of $0 < m_4 < 5$, with the values of the other parameters are as given above. When $0 < m_4 < 0.28826133$ the equilibrium E^* is stable (all eigenvalues have negative real parts). When $m_4 \approx m_{4cr1} = 0.28826133$ a complex conjugate pair becomes purely imaginary and the equilibrium loses stability through Hopf-bifurcation and becomes unstable giving rise to limit cycle which is orbitally stable (first Lyapunov coefficient is negative). For $0.28826133 < m_4 < 3.3198113$ the equilibrium, E^* unstable (two eigenvalues have positive real parts). However, when $m_4 \approx m_{4cr2} = 3.3198113$ the system again experiences Hopf-bifurcation (supercritical). For $3.3198113 < m_4 < 5$, E^* is again stable (all eigenvalues have negative real parts).

Now, we investigate the effect of m_1 . As m_1 increases from 0 to 8 two Hopf bifurcations are observed. When $0 < m_1 < 0.16385636$ we have unstable branches (two eigenvalues are positive and two have negative real parts). At $m_1 \approx m_{1cr1} = 0.16385636$ a complex conjugate pair becomes purely imaginary giving rise to the first Hopf point (supercritical). For $0.16385636 < m_1 < 6.583927$ we observe a stable branch (all eigenvalues have negative real parts). Again at $m_1 \approx m_{1cr2} = 6.583927$ two eigenvalues becomes purely imaginary giving rise to second Hopf point (supercritical). As $6.583927 < m_1 < 8$ we again observe an unstable branch (two eigenvalues are positive and two have negative real parts). Thus in the present system and for the given parameter values we observe two Hopf-bifurcations, one is stabilizing and other is destabilizing the equilibrium E^* .

Next we draw a Hopf bifurcation curve in (m_1, m_4) plane (c.f. Fig. 4) from first Hopf point ($m_4 \approx m_{4cr1} = 0.28826133$) in order to detect bifurcations with codimension-2 [23]. No codimension-2 bifurcation is observed. We also performed the continuation of the limit cycle from the first Hopf point when m_1, m_4 are treated as the free parameters. At $m_1 = 1.2$ and $m_4 = 0.28826131$ Limit point cycle is observed. Limit Point Cycle (LPC) is a fold bifurcation of the cycle from the family of limit cycles bifurcating from the Hopf point, where two limit cycles with different periods are present near LPC point. No other bifurcation point was found in this curve. Identical results were obtained when we carried out the continuation of limit cycles from other Hopf point and hence are not reported. **Our simulation results can be compared to the results given by [47]. They derived a critical value with respect to the mobility rate and found that when mobility rate is larger than critical value outbreak occurs before it dies out.**

Now, suppose that initially city 1 and 2 are disjoint (zero mobility), and that the disease is present in city 1, while city 2 is such that the disease is absent. For the parameter values given in Table 1 we find that $(R_{01}^{ODE})_{isolated} = \frac{\beta_1 K_1}{a_1(K_1 + c_1)} > 1$ while $(R_{02}^{ODE})_{isolated} = \frac{\beta_2 K_2}{a_2(K_2 + c_2)} < 1$. Now we connect both the cities. We observe that mobility can stabilize or destabilize the DFE. We observe that when we set migration $m_1 = 1.2, m_2 = 0.2, m_3 = 0.2, m_4 = 0.1$, the infection spreads in both the cities (c.f. Fig. 5(a)). The effective reproduction number for the whole network is 8.8880 greater than unity. The simulation confirms the instability of the disease-free steady state when $R_0^{ODE} > 1$. Moreover, when we set migration $m_1 = 1.2, m_2 = 3.2, m_3 = 0.2, m_4 = 3.1$, the infection is dies out in both the cities (c.f. Fig. 5(b)). In this case, the effective reproductive number is 0.719094 which is less than unity for the whole network. A change in mobility can induce a bifurcation from $R_0^{ODE} < 1$ to $R_0^{ODE} > 1$ or vice-versa. Therefore, parameters m_i can play an important role in disease controlling.

5.2 Numerical simulation for spatial model

We check the above result for our spatial model system (13)-(16) without and with spatial heterogeneity. To examine the spatio-temporal dynamics of the system, we carry out intensive numerical simulations for model (13)-(16) in two-dimensional spaces using finite difference scheme for the 2D Laplacian.

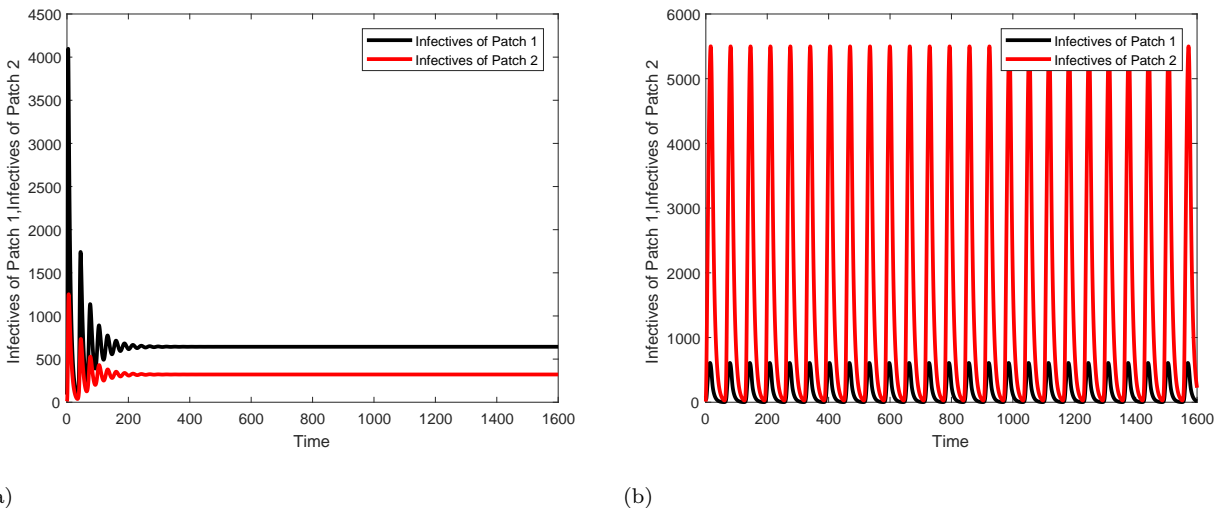


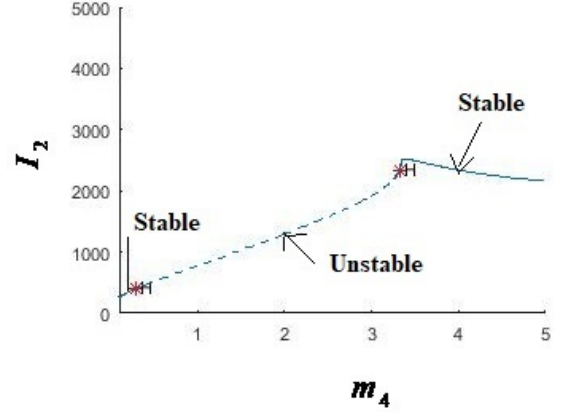
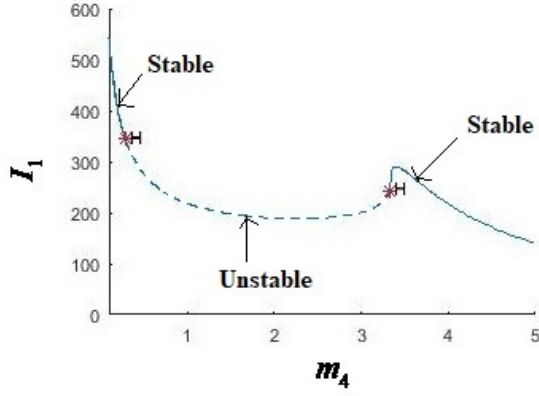
Fig. 2 Numerical simulation of the system (1)-(4), (a) Time series for infectives in both cities showing global stability of E^* with $m_4 = 0.1$, (b) Time series for infectives showing periodic dynamics in two cities with $m_4 = 3.1$. Other parameter values are the same as given in text.

We consider two cities to be identical square domains. All our numerical simulations use zero-flux or Neumann boundary conditions and nonzero initial conditions. We discretize the system of size 200×200 through $x \rightarrow (x_0, x_1, x_2, \dots, x_N)$ and $y \rightarrow (y_0, y_1, y_2, \dots, y_N)$, with $N = 800$ i.e. the spacing between the lattice points is $\Delta h = 0.25$. In the present study, we set $\Delta t = 0.001$.

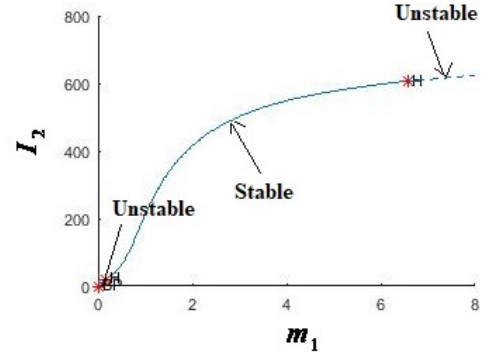
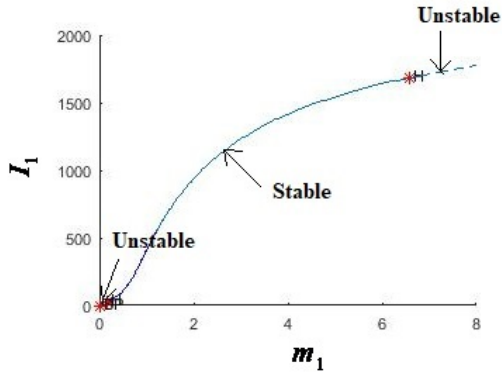
5.2.1 The effect of mobility

We confirm numerically that if the parameters and the diffusion coefficient are constant the reproduction number is the same as in the ODE case. Again, we suppose that cities 1 and 2 are isolated, and initially the disease spreads in city 1 while city 2 is such that the disease is absent, i.e., $R_{01}^{PDE} \approx 14.304723 > 1$ while $R_{02}^{PDE} \approx 0.455555 < 1$. Now, let us connect the cities. We observe that when we set migration $m_1 = 1.2, m_2 = 0.2, m_3 = 0.2, m_4 = 0.1$, the infection spreads in both the cities (c.f. Fig. 6(a)). The effective reproductive number for the coupled PDE system is $R_0^{PDE} \approx 8.9035 > 1$. However, when we set more strong migration rate $m_1 = 1.2, m_2 = 3.2, m_3 = 0.2, m_4 = 3.1$, the infection dies out in both the cities (c.f. Fig. 6(b)). The effective reproductive number for the coupled PDE system is $R_0^{PDE} \approx 0.7968 < 1$. We observe that the value of R_0^{PDE} is almost the same as in the ODE case which is in agreement with the result of Theorem 1.

Now, we are interested in studying the effect of heterogeneity. To capture the seasonality of school contacts, the transmission rate β_1 and β_2 can be set to be the periodic function. For this, we consider $\beta_1 = 2.15(1 + \cos((\pi xy)/10))$ and $\beta_2 = 0.98(1 + \cos((\pi xy)/10))$, and keep other parameters the same as above. There is no explicit formula for computing the basic reproduction number R_0^{HPDE} in a spatially heterogeneous infection. Thus, we numerically compute it by using solvepdeeig MATLAB function. If the cities are disconnected, we find $R_{01}^{HPDE} \approx 23.037539$ while $R_{02}^{HPDE} \approx 0.748634 < 1$. When the cities are connected, we observe that the disease spreads in both the cities with small population dispersal and it requires a stronger dispersal rate to reach disease-free state. Even for the migration rate $m_1 = 1.2, m_2 = 3.2, m_3 = 0.2, m_4 = 3.1$, we found $R_0^{HPDE} \approx 1.290126 > 1$ which implies that the infection does not die out in both the cities (c.f. Fig. 7(a)) which was not the case in ODE and spatial model without heterogeneity. From these simulations, we have two implications, (i) the risk of infection could be underestimated if we compute basic reproduction number using constant parameters, (ii) more stronger migration rate from disease endemic city to disease free city is required to achieve overall disease free state in spatially heterogeneous domain (c.f. Fig. 7(b)). **In contrast, [47] showed that the epidemic will die in the first community when the mobility rate is too low. Also, if mobility rate is high enough the epidemic can spread into second community before it die.**



(a)



(b)

Fig. 3 A branch of equilibria displaying existence of Hopf-bifurcations, (a) in the (m_4, I_1) and (m_4, I_2) -plane, (b) in the (m_1, I_1) and (m_1, I_2) -plane. Other parameter values are the same as given in text. H: denote a Hopf point.

Conclusion: Figure 5, 6, 7 give an overview of the dynamics of the basic reproduction number with respect to the mobility of the susceptible and infected individuals from City 1 (disease endemic) to City 2 (disease free). These figures show that if the dispersal rate from endemic to disease free city (m_2 and m_4) increases it can bring effective reproduction numbers down below unity.

5.2.2 Disease dissemination with varying diffusion

In this subsection, we investigate the influence of diffusion coefficients on R_0^{HPDE} and hence on disease prevalence or absence. Here, we fix the parameter values $D_{S_1} = 1, D_{S_2} = 5, D_{I_2} = 0.05, \beta_1 = 2.15(1 + \cos(\pi xy/10)), \beta_2 = 0.98(1 + \cos(\pi xy/10))$ and other parameter values given in Table 1 and

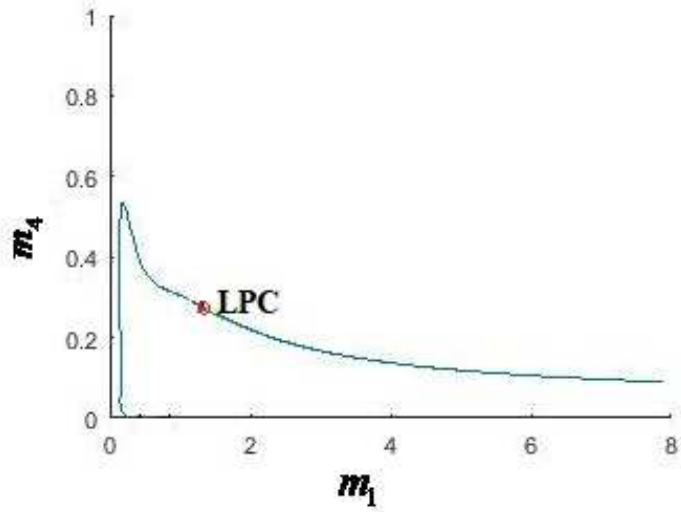


Fig. 4 The Hopf bifurcation curve in (m_1, m_4) plane. LPC: denote limit point cycle.

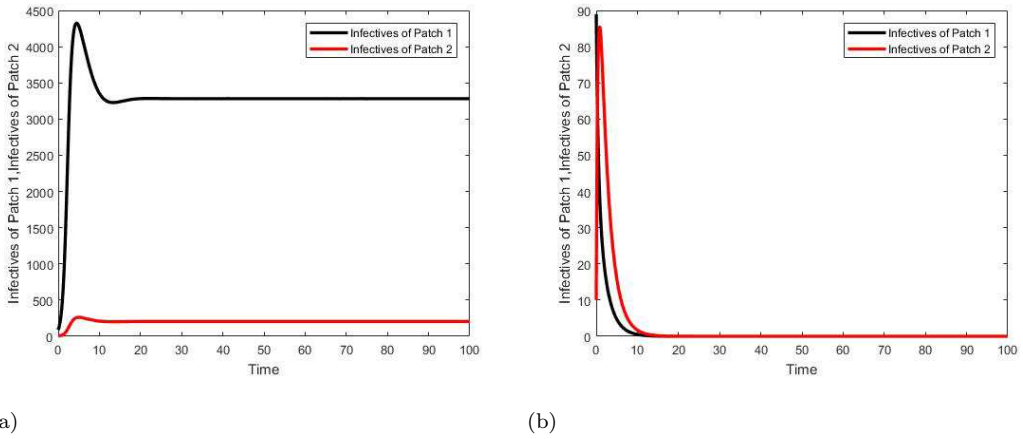


Fig. 5 (a) Time series for infectives showing the disease is sustained in two cities when $m_1 = 1.2, m_2 = 0.2, m_3 = 0.2, m_4 = 0.1$, (b) Time series for infectives showing disease is disappearing in both cities when $m_1 = 1.2, m_2 = 3.2, m_3 = 0.2, m_4 = 3.1$. Other parameter values are the same as those listed in Table 1.

vary parameter D_{I_1} . Our numerical computations signify that R_0^{HPDE} decreases as D_{I_1} increases and the system undergoes a transition from $R_0^{HPDE} > 1$ to $R_0^{HPDE} < 1$ as D_{I_1} varies from 0.01 to 10 (c.f. Fig. 8). Similarly, R_0^{HPDE} decreases as any other diffusion coefficient increases. Hence, the larger the local random diffusion, the smaller is the infection risk.

The finding is in accordance with the previous work [62]. They showed that when the agents move with a high velocity the inhomogeneity of epidemic spreading decreases. Similar results were found in [57] for a time-delayed reaction-diffusion model of dengue fever. However, recently [48] showed that monotonicity of R_0^{HPDE} with respect to diffusion rates does not hold in general. Moreover, we also observe a change in pattern formation as diffusion coefficient changes from $D_{I_1} = 0.01$ to $D_{I_2} = 10$. Infected population of city 1 gathers into large cluster at $D_{I_2} = 10$.

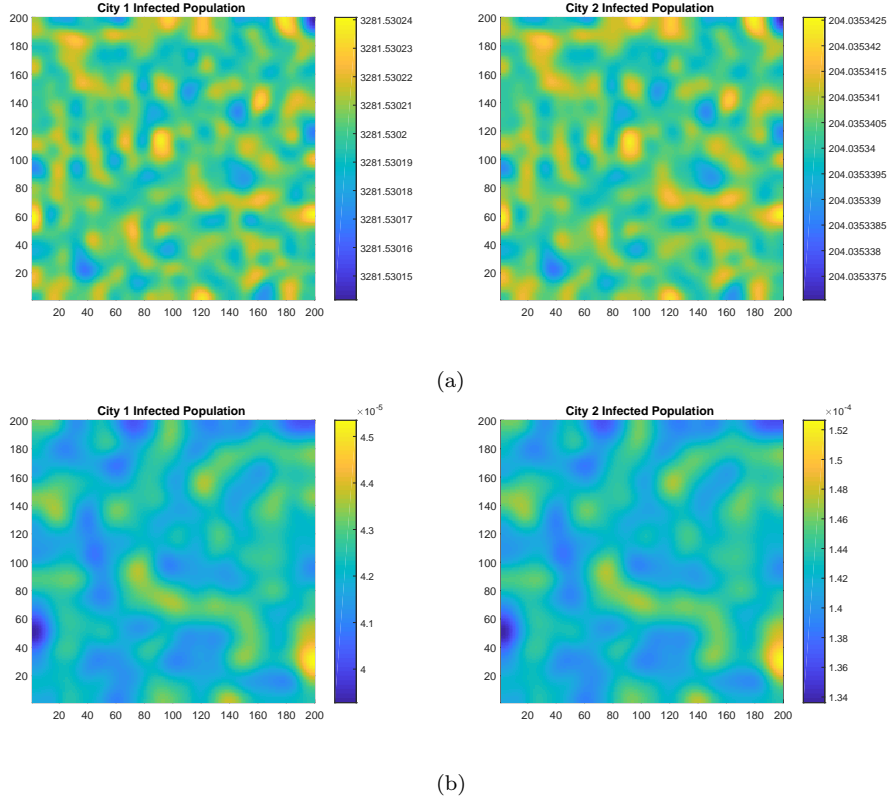


Fig. 6 Spatial dynamics for the homogeneous system (13)-(16) varying migration coefficient m_2, m_4 at $t = 100$ days, (a) $m_2 = 0.2, m_4 = 0.1$ with $R_0^{PDE} \approx 8.9035 > 1$, (b) $m_2 = 3.2, m_4 = 3.1$ with $R_0^{PDE} \approx 0.79688 < 1$. Initial conditions and other parameter values are the same as those listed in Table 1. Blue color represents minimum density and yellow color represents maximum density.

5.2.3 The effect of spatial heterogeneity

Next, we take $\beta_1 = 2.15(1 + p\cos(\pi xy/10))$ and $\beta_2 = 0.98(1 + p\cos(\pi xy/10))$, where $0 < p \leq 1$ can be interpreted as an order of magnitude of infection heterogeneity. We now fix $D_{I_1} = 0.01$ and other parameters as above. Our numerical computation indicates that if p is increased from 0 to 1 i.e. more heterogeneity of spatial infection, R_0^{HPDE} increases as a function of p . We calculate the value of R_0^{HPDE} numerically and found that for (i) $p = 0.1$, $R_0^{HPDE} \approx 0.876137 < 1$, (ii) $p = 0.4$, $R_0^{HPDE} \approx 1.113995 > 1$, (iii) $p = 0.8$, $R_0^{HPDE} \approx 1.431082 > 1$. These simulation shows that infection risk become more intense by heterogeneous spatial disease transmission (c.f. Fig. 9).

Our simulation result are in agreement with [42]. They modified the standard SIRS model on WS small-world network and BA scale-free network and analysed the model theoretically and performed computer simulation on different networks. They found that on increasing the number of links the critical value to contact rate (λ_c) decreases, i.e. for contact rate λ critical value to contact rate, infection spreads and becomes persistent. Our simulation result also shows that an increase in heterogeneity (that can be compared to increase in nodes) increases the infectives. However, we did not consider vaccination effect in controlling the epidemic propagation and can be an important factor.

6 Conclusions and discussions

A complete analysis of a two-city reaction-diffusion model is presented to study the spread dynamics of transmission of epidemics, where the parameters are distinct for both the cities. We showed that when the coupled reaction-diffusion system is at an equilibrium and city 1 has disease endemic situations, the city 2 (connected to city 1 directly or indirectly) will be also at an disease endemic level. These conclusions assume that the entire coupled system is at a steady state equilibrium. The formula for

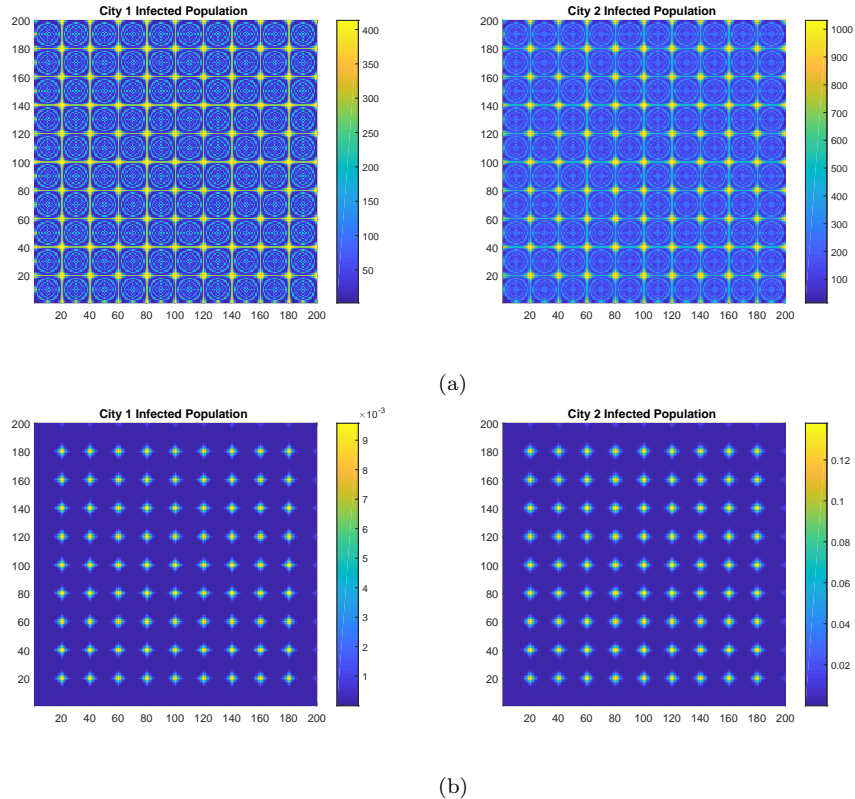


Fig. 7 Spatial dynamics for the heterogeneous system (13)-(16) with $\beta_1(x, y) = 2.15(1 + \cos(\pi xy/10))$, $\beta_2(x, y) = 0.98(1 + \cos(\pi xy/10))$ and varying migration coefficient m_2, m_4 at $t = 100$ days, (a) $m_2 = 3.2, m_4 = 3.1$ with $R_0^{HPDE} \approx 1.290126$, (b) $m_2 = 7.2, m_4 = 7.1$ with $R_0^{HPDE} \approx 0.88655 < 1$. Initial conditions and other parameter values are the same as those listed in Table 1. Blue color represents minimum density and yellow color represents maximum density.

calculating basic reproduction number R_0^{HPDE} for two city reaction-diffusion models is derived using previous findings. This formula permits us to suggest some control measures against disease spread from one city to another and to investigate the effectiveness of present public health policies. The disease free equilibrium (DFE) is globally asymptotically stable if the basic reproduction number for ODE (R_0^{ODE}) is less than unity i.e. $R_0^{ODE} \leq 1$, and unstable if $R_0^{ODE} > 1$. The health impact and consequences produced by population migration is directly related to two basic factors, (i) the distance between source and the destination [50], and (ii) the size of the mobile population migrating between different disease prevalent cities. We found the existence of codimension-1 bifurcations (two Hopf-points and Limit Point of Cycles) and discussed how endemic equilibrium, E^* changes its stability through Hopf-bifurcations. We have also shown that a population migration results in the spread of the disease in both cities, even though the disease is not prevalent in one isolated city. We also observed that a more strong population dispersal rate from disease endemic city to disease free city can bring the entire system to disease free situation.

Moreover, for spatially homogeneous infections i.e. if all parameters are constant, we demonstrated numerically that the diffusion coefficients D_{I_1} and D_{I_2} has no effect on the value of the basic reproduction number. Although, in a spatially heterogeneous environment, the random diffusion coefficients D_{I_1} and D_{I_2} affects the basic reproduction number. We notice that more local random movements among the population reduces the basic reproduction number. Alternatively, more spatial heterogeneity induces higher R_0^{HPDE} and as a result more infection risk. Numerical simulation shows that infection risk can be understated if spatially constant parameters are used to calculate basic reproduction number.

Comparative degrees of analysis are required to see the effect of traveling between and within the cities on R_0^{HPDE} , and consequently on control strategies. There are a large number of possibilities to extend the present two-city model, in order to quantify the practicality. Complex network provides a powerful platform to study the role of heterogeneous topology such as a small world, scale free and is

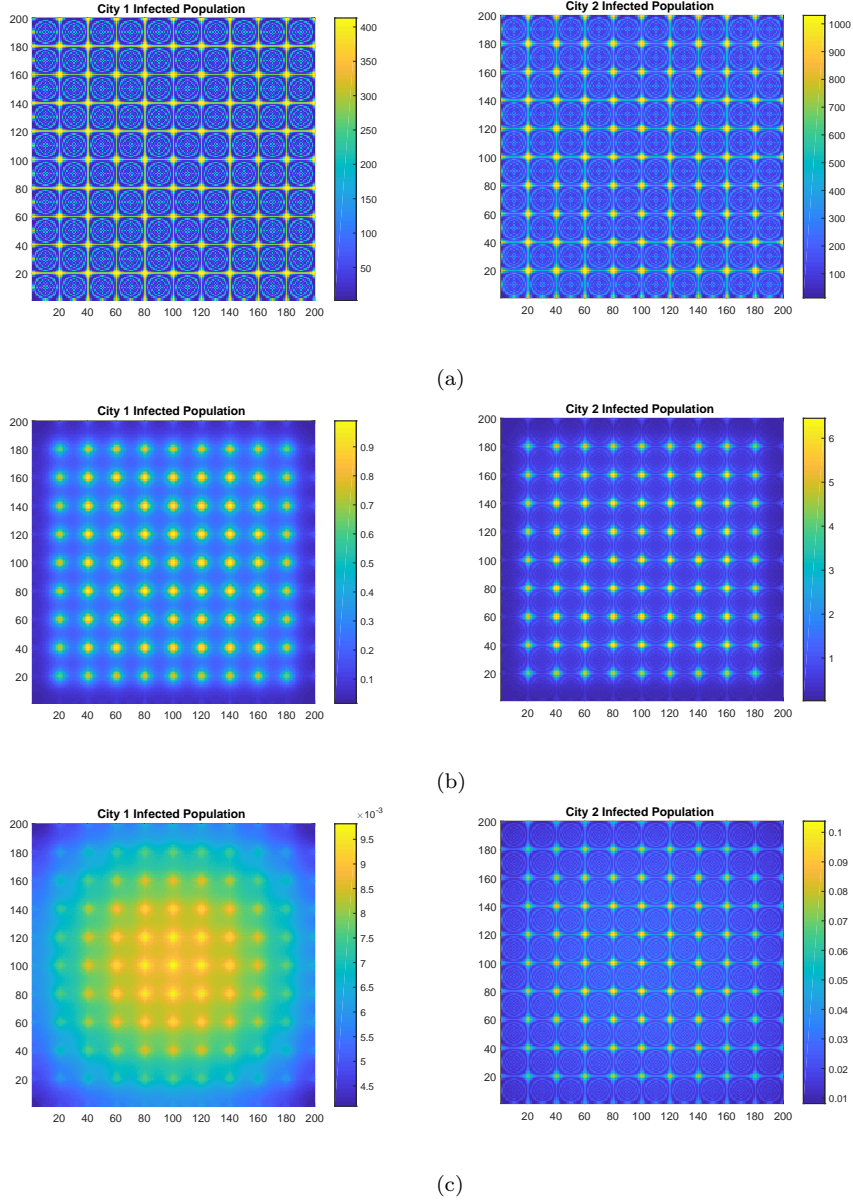


Fig. 8 Spatial dynamics of the system (13)-(16) varying diffusion coefficient D_{I_1} at $t = 300$ days, (a) $D_{I_1} = 0.01$, (b) $D_{I_1} = 1$ and (c) $D_{I_1} = 10$. Other parameter values are the same as those listed in Table 1. These figures indicate R_0^{HPDE} is decreasing function of D_{I_1} .

ignored traditionally. Analytic solution for the complete model is complicated, however the numerical solutions can be used to plan control strategies, for instance by adjusting migration parameters. The development and analysis of such reaction-diffusion network models are still in their beginning. It is worthy to note that in this work we assume that the displacements are made from a point of the first city to exactly the symmetrical point of the other. To generalize it, we have to consider an integral term to allow individuals to go to desired point in the other city. This issue will be addressed in our forthcoming work and can assist us to understand spatial spread of an epidemic more accurately when populations migrate from one location of a city to another city randomly.

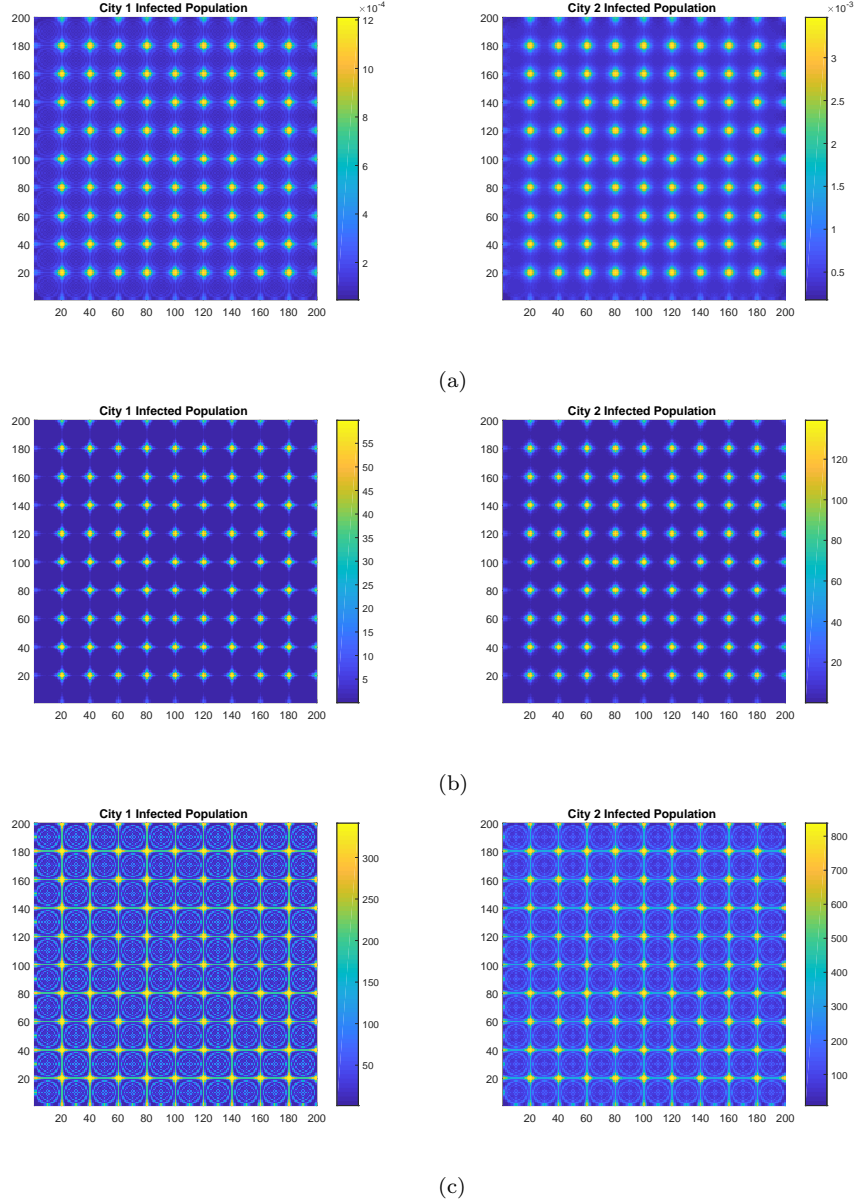


Fig. 9 Spatial dynamics of the system (13)-(16) varying magnitude of infection heterogeneity p where $\beta_1 = 2.15(1 + p\cos(\pi xy/10))$ and $\beta_2 = 0.98(1 + p\cos(\pi xy/10))$ at $t = 300$ days, (a) $p = 0.1$ with $R_0^{HPDE} \approx 0.876137 < 1$, (b) $p = 0.4$ with $R_0^{HPDE} \approx 1.1139949 > 1$ and (c) $p = 0.8$ with $R_0^{HPDE} \approx 1.431082$. Other parameter values are the same as those listed in Table 1. These figures indicate R_0^{HPDE} is an increasing function of p .

Acknowledgments

This work is supported by Normandie region France and XTerm ERDF project (European Regional Development Fund) on Complex Network and Applications.

A Appendix

Proof of proposition 5. We consider the following auxiliary system

$$-D_{S_1} \nabla^2 S_1 = (\theta r_1(x) + (1 - \theta)r_{10})S_1 \left(1 - \frac{S_1 + I_1}{K_1}\right) - \frac{(\theta\beta_1(x) - (1 - \theta)\beta_{10})S_1 I_1}{S_1 + I_1 + c_1}, \quad (74)$$

$$-D_{I_1} \nabla^2 I_1 = \frac{(\theta\beta_1(x) - (1 - \theta)\beta_{10})S_1 I_1}{S_1 + I_1 + c_1} - (\theta a_1(x) - (1 - \theta)a_{10})I_1, \quad (75)$$

$$\frac{\partial S_1}{\partial \nu} = \frac{\partial I_1}{\partial \nu} = 0.$$

where $r_{10}, \beta_{10}, a_{10}$ are positive constant and the parameter $\theta \in [0, 1]$. Problem (74)-(75) becomes problem (47) at $\theta = 1$. We divide the proof into three parts for easy understanding.

Step 1. We find the upper bounds for any positive solution (S_1, I_1) to (74)-(75). In view of (74), it holds

$$\int_{\Omega} S_1 dx \leq K_1 \quad \text{and} \quad \int_{\Omega} I_1 dx \leq K_1. \quad (76)$$

Thus, we can find a positive constant C independent of $\theta \in [0, 1]$ such that

$$(\theta r_1(x) + (1 - \theta)r_{10})S_1 \left(1 - \frac{S_1 + I_1}{K_1}\right) \leq \max(\max_{x \in \Omega} r_1(x), r_{10}) \int_{\Omega} S_1 dx \leq C$$

and

$$(\theta\beta_1(x) + (1 - \theta)\beta_{10}) \frac{S_1 I_1}{S_1 + I_1 + c_1} \leq \max(\max_{x \in \Omega} \beta_1(x), \beta_{10}) \int_{\Omega} I_1 dx \leq C$$

The positive constant C does not depend on the parameter $\theta \in [0, 1]$ and can be different depending on its position. Applying L^1 estimate theory for elliptic equations [5] to equations (74)-(75), we obtain $\|S_1\|_{W^{1,1}(\Omega)} \leq C$ and $\|I_1\|_{W^{1,1}(\Omega)} \leq C$. Application of Sobolev embedding theorem gives us,

$$W^{1,1}(\Omega) \rightarrow L^p(\Omega), \quad \forall 1 \leq p \leq \frac{n}{n-1} \quad \text{or} \quad 1 \leq p < \infty \quad \text{if} \quad n = 1.$$

we have

$$\|S_1\|_{L^p(\Omega)}, \|I_1\|_{L^p(\Omega)} \leq C, \quad \forall 1 \leq p \leq \frac{n}{n-1} \quad \text{or} \quad 1 \leq p < \infty \quad \text{if} \quad n = 1. \quad (77)$$

Applying L^p estimate for elliptic equations [13] to (74)-(75) leads to

$$\|S_1\|_{W^{2,p}(\Omega)}, \|I_1\|_{W^{2,p}(\Omega)} \leq C, \quad \forall 1 \leq p \leq \frac{n}{n-1} \quad \text{or} \quad 1 \leq p < \infty \quad \text{if} \quad n = 1. \quad (78)$$

Again we apply Sobolev embedding theorem, to get

$$\|S_1\|_{L^{p^*}(\Omega)}, \|I_1\|_{L^{p^*}(\Omega)} \leq C, \quad \forall 1 \leq p^* \leq \frac{n}{n-3} \quad \text{or} \quad 1 \leq p^* < \infty \quad \text{if} \quad n = 1. \quad (79)$$

Repeating the above process finitely many times, one can affirm that

$$\|S_1\|_{L^\infty(\Omega)} \leq C, \|I_1\|_{L^\infty(\Omega)} \leq C. \quad (80)$$

Step 2. Now, we find lower bounds for any positive solution (S_1, I_1) to (74)-(75). Integrating (75) over Ω gives

$$\int_{\Omega} [\theta\beta(x) + (1 - \theta)\beta_{10}] \frac{S_1 I_1}{S_1 + I_1 + c_1} dx = \int_{\Omega} [\theta a(x) + (1 - \theta)a_{10}] I_1 dx, \quad (81)$$

Clearly, (81) indicates

$$c \int_{\Omega} I_1 dx \leq d \int_{\Omega} S_1 dx, \quad (82)$$

where $c = \min(\min_{x \in \Omega} a(x), a_{10}) > 0, d = \max(\max_{x \in \Omega} \beta(x), \beta_{10}) > 0$. One can then insert $\int_{\Omega} I_1 dx \leq K_1 - \int_{\Omega} S_1 dx$ into (82) to get

$$\int_{\Omega} S_1 dx \geq \frac{cK_1}{c+d}. \quad (83)$$

Notice that S_1 satisfies

$$-\nabla^2 S_1 + \frac{1}{D_{S_1}} \max(\max_{x \in \Omega} \beta_1(x), \beta_{10}) S_1 > 0, \quad \forall x \in \Omega. \quad (84)$$

Thus, together with (83) and Lemma 1 with $q = 1$ concludes that

$$S_1(x) \geq C, \quad \forall x \in \Omega. \quad (85)$$

We next take $\min_{\bar{\Omega}} I_1(x) = I(x_0)$. According to [35], one can see

$$\frac{[\theta\beta_1(x_0) + (1-\theta)\beta_{10}]S_1(x_0)}{S_1(x_0) + I_1(x_0) + c_1} \leq \theta a_1(x) + (1-\theta)a_{10}. \quad (86)$$

This leads to

$$\min_{\bar{\Omega}} I_1(x) = I_1(x_0) \geq \frac{\min(\min_{\bar{\Omega}} \beta_1(x), \beta_{10})S_1(x_0)}{\max(\max_{\bar{\Omega}} a_1(x), a_{10})} - c_1 - S_1(x_0) \geq C. \quad (87)$$

If $\beta_1(x_0)S_1(x_0)/a_1(x_0) - c_1 - S_1(x_0) > 0$, from the above analysis of step 1 and 2 we can always find a positive constant $C_* > 1$, which is independent of $\theta \in [0, 1]$, such that any positive solution (S_1, I_1) of (74)-(75) satisfies

$$\frac{1}{C_*} < S_1(x), I_1(x) < C_*, \forall x \in \bar{\Omega} \quad (88)$$

Step 3. Finally, we find existence of positive solution to (74)-(75). Let us denote a set,

$$\Theta = \{(S_1, I_1) \in C(\bar{\Omega}) \times C(\bar{\Omega}) : \frac{1}{C_*} < S_1(x), I_1(x) < C_*, \} \quad (89)$$

Thus, (74)-(75) has no positive solution $(S_1, I_1) \in \partial\Theta$. For $\theta \in [0, 1]$, we also define the operator

$$H(\theta, (S_1, I_1)) = (-\nabla^2 + I)^{-1}(\hat{h}(\theta, (S_1, I_1)), \tilde{h}(\theta, (S_1, I_1))), \quad (90)$$

$$\begin{aligned} \hat{h} &= S + D_{S_1}^{-1} \left((\theta r_1(x) + (1-\theta)r_{10})S_1 \left(1 - \frac{S_1 + I_1}{K_1} \right) - \frac{(\theta\beta_1(x) - (1-\theta)\beta_{10})S_1 I_1}{S_1 + I_1 + c_1} \right), \\ \tilde{h} &= I + D_{I_1}^{-1} \left(\frac{(\theta\beta_1(x) - (1-\theta)\beta_{10})S_1 I_1}{S_1 + I_1 + c_1} - (\theta a_1(x) - (1-\theta)a_{10})I_1 \right), \end{aligned} \quad (91)$$

Clearly, the existence of positive solutions of (47) is identical to the existence of fixed point of the operator $H(1, \cdot)$ in Θ . From standard elliptic regularity theory one can find that H is a compact operator from $[0, 1] \times \Theta$ to $C(\bar{\Omega}) \times C(\bar{\Omega})$. Furthermore, we have

$$(S_1, I_1) \neq H(\theta, (S_1, I_1)), \forall \theta \in [0, 1] \text{ and } (S_1, I_1) \in \partial\Theta.$$

Therefore, the topological degree $\deg(I - H(\theta, \cdot), \Theta)$ is well-defined and is independent of $\theta \in [0, 1]$. Denote

$$\begin{aligned} S_{10}^* &= \frac{a_1(\sqrt{B} + (c_1 r_1 + K_1(a_1 - \beta_1 + r_1)))}{2\beta_{10} r_1} \\ I_{10}^* &= \frac{-(a_1 - \beta_1)^2 K_1 - (\beta_1(c_1 - K_1) + a_1(c_1 + K_1))r_1 + \sqrt{(a_1 - \beta_1)^2 B}}{2\beta_{10} r_1} \end{aligned}$$

where $B = (a_1 - \beta_1)K_1^2 + 2K_1(\beta_1(c_1 - K_1) + a_1(c_1 + K_1))r_1 + (c_1 + K_1)^2 r_1^2$. [55] have already proved that (S_{10}^*, I_{10}^*) is linearly stable when $\beta_1(x), r_1(x), a_1(x)$ are constant. Using well-known Leray-Schauder degree index formula, we have

$$\deg(I - H(0, \cdot), \Theta) = \text{index}(I - H(0, \cdot), (S_{10}^*, I_{10}^*)) = 1.$$

Therefore, from homotopy invariance of the Leray-Schauder degree it follows that

$$\deg(I - H(1, \cdot), \Theta) = \deg(I - H(0, \cdot), \Theta) = 1,$$

which implies that $H(1, \cdot)$ has at least one fixed point in Θ . As a consequence, (47) has at least one positive solution.

References

1. Allen, L.J., Bolker, B.M., Lou, Y., Nevai, A.L.: Asymptotic profiles of the steady states for an sis epidemic reaction-diffusion model. *Discrete and Continuous Dynamical Systems* **21**(1), 1 (2008)
2. Anderson, R.M., May, R.: *Infectious diseases of humans*. 1991. New York: Oxford Science Publication Google Scholar (1991)
3. Arino, J., Van den Driessche, P.: A multi-city epidemic model. *Mathematical Population Studies* **10**(3), 175–193 (2003)
4. Berman, A., Plemmons, R.J.: *Nonnegative matrices in the mathematical sciences*, vol. 9. Siam (1994)
5. Brézis, H., Strauss, W.A.: Semi-linear second-order elliptic equations in \mathbb{R}^n . *Journal of the Mathematical Society of Japan* **25**(4), 565–590 (1973)
6. Brockmann, D., Hufnagel, L., Geisel, T.: The scaling laws of human travel. *Nature* **439**(7075), 462 (2006)
7. Chen, W., Wang, M.: Qualitative analysis of predator-prey models with beddington-deangelis functional response and diffusion. *Mathematical and Computer Modelling* **42**(1-2), 31–44 (2005)
8. Cui, R., Lou, Y.: A spatial sis model in advective heterogeneous environments. *Journal of Differential Equations* **261**(6), 3305–3343 (2016)

9. Deng, K., Wu, Y.: Dynamics of a susceptible-infected-susceptible epidemic reaction-diffusion model. *Proceedings. Section A, Mathematics-The Royal Society of Edinburgh* **146**(5), 929 (2016)
10. Diekmann, O., Kretzschmar, M.: Patterns in the effects of infectious diseases on population growth. *Journal of Mathematical Biology* **29**(6), 539–570 (1991)
11. Van den Driessche, P., Watmough, J.: Reproduction numbers and sub-threshold endemic equilibria for compartmental models of disease transmission. *Mathematical biosciences* **180**(1-2), 29–48 (2002)
12. Fife, P.C.: *Mathematical aspects of reacting and diffusing systems*, vol. 28. Springer Science & Business Media (2013)
13. Gilbarg, D., Trudinger, N.S.: *Elliptic partial differential equations of second order*. Springer (2015)
14. Guin, L.N., Mandal, P.K.: Spatiotemporal dynamics of reaction–diffusion models of interacting populations. *Applied Mathematical Modelling* **38**(17-18), 4417–4427 (2014)
15. Hethcote, H.W.: Qualitative analyses of communicable disease models. *Mathematical Biosciences* **28**(3-4), 335–356 (1976)
16. Hethcote, H.W.: The mathematics of infectious diseases. *SIAM review* **42**(4), 599–653 (2000)
17. Huang, W., Han, M., Liu, K.: Dynamics of an sis reaction-diffusion epidemic model for disease transmission. *Mathematical Biosciences & Engineering* **7**(1), 51 (2010)
18. Jorgensen, S.E.: *Handbook of environmental data and ecological parameters*, vol. 6. Pergamon (1979)
19. Keeling, M., Rohani, P.: Modeling infectious diseases in humans and animals. *Clinical Infectious Diseases* **47**, 864–6 (2008)
20. Knuth, D.E.: *The art of computer programming, volume 4A: combinatorial algorithms, part 1*. Pearson Education India (2011)
21. Krein, M.G.: Linear operators leaving invariant a cone in a banach space. *Amer. Math. Soc. Transl. Ser. I* **10**, 199–325 (1962)
22. Kuto, K., Matsuzawa, H., Peng, R.: Concentration profile of endemic equilibrium of a reaction–diffusion–advection sis epidemic model. *Calculus of Variations and Partial Differential Equations* **56**(4), 112 (2017)
23. Kuznetsov, Y.A.: *Elements of applied bifurcation theory*, vol. 112. Springer Science & Business Media (2013)
24. Lam, K.Y., Lou, Y.: Asymptotic behavior of the principal eigenvalue for cooperative elliptic systems and applications. *Journal of Dynamics and Differential Equations* **28**(1), 29–48 (2016)
25. LaSalle, J.P.: *The stability of dynamical systems*, vol. 25. Siam (1976)
26. Lei, C., Li, F., Liu, J.: Theoretical analysis on a diffusive sir epidemic model with nonlinear incidence in a heterogeneous environment. *Discrete & Continuous Dynamical Systems-B* **23**(10), 4499 (2018)
27. Lei, C., Xiong, J., Zhou, X.: Qualitative analysis on an sis epidemic reaction-diffusion model with mass action infection mechanism and spontaneous infection in a heterogeneous environment. *Discrete & Continuous Dynamical Systems-B* **22**(11), 1 (2019)
28. Li, B., Bie, Q.: Long-time dynamics of an sirs reaction-diffusion epidemic model. *Journal of Mathematical Analysis and Applications* **475**(2), 1910–1926 (2019)
29. Li, B., Li, H., Tong, Y.: Analysis on a diffusive sis epidemic model with logistic source. *Zeitschrift für angewandte Mathematik und Physik* **68**(4), 96 (2017)
30. Li, H., Peng, R., Wang, F.B.: Varying total population enhances disease persistence: Qualitative analysis on a diffusive sis epidemic model. *Journal of Differential Equations* **262**(2), 885–913 (2017)
31. Li, H., Peng, R., Wang, Z.A.: On a diffusive susceptible-infected-susceptible epidemic model with mass action mechanism and birth-death effect: analysis, simulations, and comparison with other mechanisms. *SIAM Journal on Applied Mathematics* **78**(4), 2129–2153 (2018)
32. Li, M.Y., Shuai, Z.: Global-stability problem for coupled systems of differential equations on networks. *Journal of Differential Equations* **248**(1), 1–20 (2010)
33. Lieberman, G.M.: Bounds for the steady-state sel’kov model for arbitrary p in any number of dimensions. *SIAM journal on mathematical analysis* **36**(5), 1400–1406 (2005)
34. Liu, Z., Wang, X., Wang, M.: Inhomogeneity of epidemic spreading. *Chaos: An Interdisciplinary Journal of Nonlinear Science* **20**(2), 023128 (2010)
35. Lou, Y., Ni, W.M.: Diffusion, self-diffusion and cross-diffusion. *Journal of Differential Equations* **131**(1), 79–131 (1996)
36. Magal, P., Webb, G., Wu, Y.: On a vector-host epidemic model with spatial structure. *Nonlinearity* **31**(12), 5589 (2018)
37. Magal, P., Webb, G.F., Wu, Y.: On the basic reproduction number of reaction-diffusion epidemic models. *SIAM Journal on Applied Mathematics* **79**(1), 284–304 (2019)
38. May, R.M.: Uses and abuses of mathematics in biology. *Science* **303**(5659), 790–793 (2004)
39. McCallum, H., Barlow, N., Hone, J.: How should pathogen transmission be modelled? *Trends in ecology & evolution* **16**(6), 295–300 (2001)
40. Murray, J.: *Mathematical biology ii* 3 ed., 536 (2003)
41. Nian, F., Hu, C., Yao, S., Wang, L., Wang, X.: An immunization based on node activity. *Chaos, Solitons & Fractals* **107**, 228–233 (2018)
42. Nian, F., Wang, X.: Efficient immunization strategies on complex networks. *Journal of theoretical biology* **264**(1), 77–83 (2010)
43. Peng, R.: Asymptotic profiles of the positive steady state for an sis epidemic reaction–diffusion model. part i. *Journal of Differential Equations* **247**(4), 1096–1119 (2009)
44. Peng, R., Yi, F.: Asymptotic profile of the positive steady state for an sis epidemic reaction–diffusion model: effects of epidemic risk and population movement. *Physica D: Nonlinear Phenomena* **259**, 8–25 (2013)
45. Peng, R., Zhao, X.Q.: A reaction–diffusion sis epidemic model in a time-periodic environment. *Nonlinearity* **25**(5), 1451 (2012)
46. Protter, M.H., Weinberger, H.F.: *Maximum principles in differential equations*. Springer Science & Business Media (2012)

47. Ren, G., Wang, X.: Epidemic spreading in time-varying community networks. *Chaos: An Interdisciplinary Journal of Nonlinear Science* **24**(2), 023116 (2014)
48. Song, P., Lou, Y., Xiao, Y.: A spatial seirs reaction-diffusion model in heterogeneous environment. *Journal of Differential Equations* (2019)
49. Strauss, W.A.: *Partial differential equations: An introduction*. Wiley (2007)
50. Stürchler, D., et al.: *Endemic areas of tropical infections*. Edn 2. Hans Huber Publishers (1988)
51. Suo, J., Li, B.: Analysis on a diffusive sis epidemic system with linear source and frequency-dependent incidence function in a heterogeneous environment. *Math. Biosci. Eng.* **17**(1), 418–441 (2020)
52. Tewa, J.J., Bowong, S., Mewoli, B.: Mathematical analysis of two-patch model for the dynamical transmission of tuberculosis. *Applied Mathematical Modelling* **36**(6), 2466–2485 (2012)
53. Thieme, H.R.: Spectral bound and reproduction number for infinite-dimensional population structure and time heterogeneity. *SIAM Journal on Applied Mathematics* **70**(1), 188–211 (2009)
54. Tong, Y., Lei, C.: An sis epidemic reaction–diffusion model with spontaneous infection in a spatially heterogeneous environment. *Nonlinear Analysis: Real World Applications* **41**, 443–460 (2018)
55. Upadhyay, R.K., Roy, P., Rai, V.: Deciphering dynamics of epidemic spread: The case of influenza virus. *International Journal of Bifurcation and Chaos* **24**(05), 1450064 (2014)
56. Wang, W., Zhao, X.Q.: An epidemic model in a patchy environment. *Mathematical biosciences* **190**(1), 97–112 (2004)
57. Wang, W., Zhao, X.Q.: A nonlocal and time-delayed reaction-diffusion model of dengue transmission. *SIAM Journal on Applied Mathematics* **71**(1), 147–168 (2011)
58. Wang, W., Zhao, X.Q.: Basic reproduction numbers for reaction-diffusion epidemic models. *SIAM Journal on Applied Dynamical Systems* **11**(4), 1652–1673 (2012)
59. Wang, X., Zhao, T.: Model for multi-messages spreading over complex networks considering the relationship between messages. *Communications in Nonlinear Science and Numerical Simulation* **48**, 63–69 (2017)
60. Wang, X., Zhao, T., Qin, X.: Model of epidemic control based on quarantine and message delivery. *Physica A: Statistical Mechanics and its Applications* **458**, 168–178 (2016)
61. Wen, X., Ji, J., Li, B.: Asymptotic profiles of the endemic equilibrium to a diffusive sis epidemic model with mass action infection mechanism. *Journal of Mathematical Analysis and Applications* **458**(1), 715–729 (2018)
62. Wen-Jie, Z., Xing-Yuan, W.: Inhomogeneity of epidemic spreading with entropy-based infected clusters. *Chaos: An Interdisciplinary Journal of Nonlinear Science* **23**(4), 043105 (2013)
63. Wu, Y., Zou, X.: Asymptotic profiles of steady states for a diffusive sis epidemic model with mass action infection mechanism. *Journal of Differential Equations* **261**(8), 4424–4447 (2016)
64. Xu, Z., Ai, C.: Traveling waves in a diffusive influenza epidemic model with vaccination. *Applied Mathematical Modelling* **40**(15–16), 7265–7280 (2016)